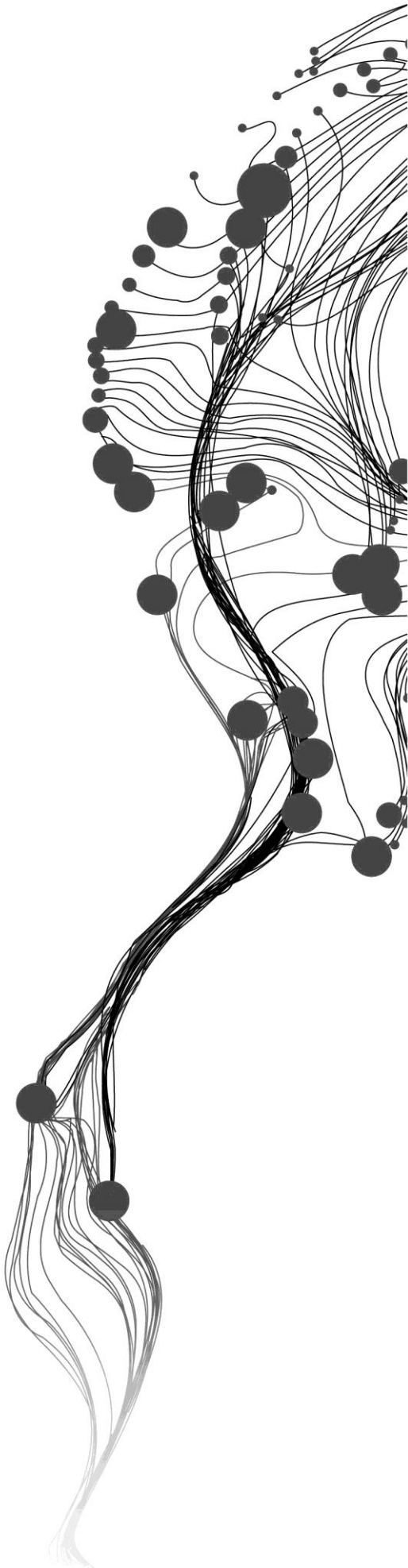


USING SATELLITE-BASED RAINFALL ESTIMATES FOR RUNOFF MODELLING WITH THE REW APPROACH: THE CASE OF UPPER GILGEL ABAY CATCHMENT

ASSAYEW NEBERE AMBAW
February, 2016

SUPERVISORS:
Dr.Ing. T.H.M. Rientjes
Ir. G.N. Parodi



Using satellite-based rainfall estimates for runoff modelling with the REW approach: the case of Upper Gilgel Abay catchment

ASSAYEW NEBERE AMBAW

Enschede, The Netherlands, February, 2016

Thesis submitted to the Faculty of Geo-Information Science and Earth Observation of the University of Twente in partial fulfilment of the requirements for the degree of Master of Science in Geo-information Science and Earth Observation.

Specialization: Water Resources and Environmental Management

SUPERVISORS:

Dr. Ing. T.H.M. Rientjes

Ir. G.N. Parodi

THESIS ASSESSMENT BOARD:

Dr. M.W. Lubczynski (Chair)

Prof. P. (Paolo). Regianni (External Examiner, University of Siegen)

DISCLAIMER

This document describes work undertaken as part of a programme of study at the Faculty of Geo-Information Science and Earth Observation of the University of Twente. All views and opinions expressed therein remain the sole responsibility of the author, and do not necessarily represent those of the Faculty.

ABSTRACT

A physically based hydrological modeling approach, Representative elementary watershed (REW), has been applied to the Upper Gilgel Abay catchment which is the largest contributor to the inflow to Lake Tana, the source of Blue Nile River. Application and evaluation of performances of satellite rainfall estimates (SRE) for representing the spatial and temporal variability of rainfall in data poor catchments such as Upper Gilgel Abay is vital. Rainfall variability was reported within Upper Gilgel Abay catchment between mountainous areas and flat areas close to the Lake. The important component which is associated with variability of rainfall is the runoff dynamics and generation mechanisms in Upper Gilgel Abay catchment. Hence, the focus of this study was to test the effectiveness satellite rainfall estimates at high spatial and temporal resolutions for simulating spatial dynamics of runoff in Upper Gilgel Abay catchment.

The study period of 2006-2010 was used for downloading the 1-hr temporal and 8 km × 8 km spatial resolution CMORPH data (selected from SREs), and extracting SRE. SREs are constrained for use because of the systematic and random errors over space and time. For correcting the systematic biases, time and space variant bias correction algorithm was applied for a time window of 7 days and a minimum rain accumulation of 5 mm within these days. Bias correction selected for this study aimed at correcting both in space and time domains. To estimate potential evapotranspiration for model inputs Penman-Monteith equation was calculated from climatological and field measurements. TARDEM software was used in the model for extracting the REWs and performing hydro processing from SRTM DEM with a resolution of 90 m. The model was calibrated for the period 2006-2008 using rainfall data from the rain gauges. Calibration was conducted in trial and error through parameter optimization. After getting the better performing model results the precipitation forcing was replaced with CMORPH inputs. Objective functions like NS, RVE and Y were applied to assess how well the stream flows were reproduced in simulations. Hourly CMORPH based simulations were used as modeling time step to simulate the diurnal variability of streamflow in Upper Gilgel Abay catchment. The result was evaluated through visual inspection and Exceedance probability plots.

Based on modeling results, objective function values for calibration are 0.71 for NS, 4.07% for RVE and 0.68 for Y. Values as such indicate a satisfactory model performance. The sensitivity analysis results show hydraulic conductivities, soil porosity and depth of saturated subsurface flow layer are highly sensitive in affecting the simulation results. Objective function values of 0.57 for NS, 0.80% for RVE and 0.56 for Y was reported while using CMORPH SRE inputs instead of Insitu rainfall estimates. Thus, Insitu based simulation has better reproduced the measured streamflow hydrograph than CMORPH based streamflow simulations. A validation result of 0.62 for NS, 9.59% for RVE and 0.57 for Y was found and the validation results deteriorated from the calibration results. The daily aggregated CMORPH simulation suppresses the high peak flows and low flows when compared to the hourly CMORPH. Regarding saturated excess overland flow, the spatial differences in signals identified in Upper Gilgel Abay catchment where REWs close to the river reaches and areas of flat terrain contribute higher to streamflow by saturation excess overland.

Overall, the performance of SREs based streamflow simulations was able to capture the shape of stream flow hydrograph measured. Model recalibration with SRE forcing might improve the model performance even better.

KEY WORDS: REW; CMORPH; Satellite rainfall estimates; runoff; modelling

ACKNOWLEDGEMENTS

First and foremost I would like to thank God for his mercy all the way through my life.

I would like to express my sincere gratitude to the government of the Netherlands for providing me this great opportunity to study under the Netherlands fellowship program.

I consider it a profound pleasure to express my deep sense of indebtedness, gratitude and profound thanks to first supervisor Dr.Ing T.H.M. Rientjes, for his valuable comments and guidance throughout the research. His comments and helpful guidance gave me a chance to explore further. I have learned a lot from him.

I would also like to give great gratitude to Ir. G.N. Parodi my second supervisor, for his supportive and valuable comments.

I would thankfully acknowledge Ministry of Water Resources and Bahir Dar Meteorological Services Agency in Ethiopia for providing hydro-meteorological data for the study.

I would gratefully like to acknowledge University of Gondar for allowing me to pursue my studies abroad.

I would also like to extend my deepest gratitude to my friends, colleagues in ITC, WREM department staffs in ITC, and GeES Department staffs in University of Gondar.

I am forever grateful to my beloved Father Nebere Ambaw. He had always been the constant source of my strength and hope in every aspect of my life. My special heartfelt gratitude also goes to my beloved wife Sosina Mihret, my mother Simegn Alemu and my brother Getaye Nebere for their affection and encouragement.

TABLE OF CONTENTS

1. Introduction	1
1.1. Background	1
1.2. Problem Statement	2
1.3. Main objective	2
1.3.1. Specific objectives	2
1.3.2. Research questions	3
1.4. Relevance of the study	3
1.5. Thesis outline.....	3
2. study area and data availability	4
2.1. Study area description	4
2.1.1. Geographical location and topography	4
2.1.2. Climate	5
2.1.3. Land use/Land cover, Soil and Geology.....	6
2.2. Data Availability	7
2.2.1. Insitu measurement.....	7
2.2.1.1. Meteorological Variables	7
2.2.1.2. Hydrological Data.....	8
2.2.2. Remote sensing data	9
3. Literature review	10
3.1. Sattelite rainfall estimates as forcing for Modeling runoff.....	10
3.2. Runoff processes.....	11
3.3. Hydrograph components.....	13
4. Methodology	14
4.1. Methodological approach	14
4.2. Processing satellite rainfall estimates	15
4.2.1. Extraction of SREs	15
4.2.2. Bias correction scheme.....	15
4.3. Comparison of stream flow simulation using rainfall forcing of daily and hourly CMORPH	16
4.4. Filling in techniques used for missing gauge measurements	16
4.5. Penman-Monteith equation for Potential Evaporation	17
4.6. Digital elevation model (DEM) processing.....	18
4.7. Model description	19
4.8. Balance equations at the REW-scale	21
4.9. Parameters and variables.....	22
4.10. Evaluation of model performance	23
5. Result and Discussion	24
5.1. Performance of satellite rainfall estimates (SREs) in Upper Gilgel Abay Catchment	24
5.1.1. Performance of CMORPH	24
5.1.2. Effects of Bias correction	26
5.2. REW modelling.....	27
5.2.1. Calibration and Validation.....	27

5.2.1.1.	Model calibration	28
5.2.1.2.	Sensitivity Analysis	29
5.2.1.3.	Model Validation	30
5.3.	Runoff simulation with satellite rainfall estimates forcing	31
5.4.	Identification of major runoff source within the catchment	32
5.5.	Comparison of high temporal resolution (hourly) and daily forcing on runoff simulation	35
5.6.	Discussion	37
6.	Conclusion and Recommendation	40
6.1.	Conclusions	40
6.2.	Recommendations	41

LIST OF FIGURES

Figure 1: Location of Upper Gilgel Abay catchment	4
Figure 2: Elevation map of Upper Gilgel Abay catchment	5
Figure 3: Basin averaged daily rainfall of Upper Gilgel Abay catchment (2006-2010).....	5
Figure 4: Average daily temperature of Upper Gilgel Abay catchment (2006-2010)	6
Figure 5: Location of meteorological and gauging stations considered in Upper Gilgel Abay catchment	8
Figure 6: Annual rainfall of Upper Gilgel Abay catchment for meteorological stations	8
Figure 7: Discharge measurement taken in the outlet of Upper Gilgel Abay catchment.....	9
Figure 8: classification of runoff generation mechanisms (Source: Tarboton (2003) adapted from (Beven, 2000)).....	11
Figure 9: Typical surface with saturation excess (exfiltration) in the Upper Gilgel Abay catchment (photo: Dr.Ing. T.H.M. Rientjes).	12
Figure 10: stream flow hydrograph (from public resource GeogOnline)	13
Figure 11: Flowchart showing the procedures and methods.....	14
Figure 12: Characteristics of the hypothetical reference crop (Source: (Allen, 1998)).....	17
Figure 13: REWs delineated with Second Strahler order.....	18
Figure 14: Discretization of the Upper Gilgel Abay river catchment in to 33 REWs (Left) and 173 REWs (Right) based on Strahler order used.....	19
Figure 15: Three-dimensional view of REW model (Source:(Reggiani & Rientjes, 2005)).....	20
Figure 16: REW cross-section and mass exchange terms (source: (Fenicia et al., 2005)).....	20
Figure 17: Scatter plots of CMORPH and gauge daily rainfall (2006-2010).....	25
Figure 18: Whisker plot showing comparison of BF'S obtained from 7 days sampling window (2006-2010)	26
Figure 19: Hydrograph showing the calibration result for 2006-2008.....	29
Figure 20: validation hydrograph for the year 2009	30
Figure 21: Streamflow simulation with bias orrected CMORPH rainfall estimates (2006-2010).....	31
Figure 22: Stream flow simulation with bias corrected CMORPH rainfall estimate (left; for the year 2008; and right; 2010)	32
Figure 23: Average Saturation excess thickness (mm) for REWs for wet season (months of June, July, August and September 2006-2008) per day.....	33
Figure 24: major runoff generation (saturation excess) source REWs	33
Figure 25: Simulated saturated excess overland flow thickness for REW 4, REW 13, and REW 25.....	34
Figure 26: Correlation of REW average daily rainfall and Simulated saturated excess overland flow for REW 4, REW 13, and REW 25	34
Figure 27: Comparison of hourly and the daily forcing on runoff simulation (June, July and August 2010)	35
Figure 28: Exceedance probability graph.....	36
Figure 29: Streamflow simulation with bias corrected CMORPH and Insitu rainfall estimates(2006-2008)	38

LIST OF TABLES

Table 1: Shows meteorological variables collected for this study.....	7
Table 2: Summary of Mass balance equations in REW model (Reggiani & Rientjes, 2005).....	21
Table 3: Summary statistics of gauge and CMORPH daily rainfall (2006-2010)	24
Table 4: Summary statistics of CMORPH daily rainfall before and after TSV bias correction	27
Table 5: Sensitivity analysis (2006-2008).....	30
Table 6: Performance of CMORPH on runoff simulation	31

1. INTRODUCTION

1.1. Background

Gilgel Abay catchment is of high interest to Ministry of Water Resources and Energy in Ethiopia because the basin is the head basin of the Upper Blue Nile and the largest contributor to Lake Tana which is responsible for some 30% of the mean annual lake inflow. Lake Tana is also the actual source of the Upper Blue Nile. Hence in recent years, the basin has received much attention from scientists. Most studies performed in the catchment are on rainfall-runoff modelling with the aim to better understand and simulate the hydrological regime. Applications are known for the HBV conceptual model by Wale (2008), Uhlenbrook et al. (2010) and Rientjes et al. (2011), and the semi-distributed conceptual model (TOPMODEL) by Moges (2008), Ahmed (2012) and Gumindoga (2015). Other studies known are on Lake Tana water balance modelling by Wale (2008) and Rientjes et al. (2011); and on hydrological impact assessments of land cover changes in Gilgel Abay by Moges (2008), Ahmed (2012) and Gumindoga (2015); Studies on climate change impact assessment on the hydrology of the catchment are by Abdo et al. 2009 and Yihun et al. 2013. Uhlenbrook et al. (2010) and Dessie et al. (2014) also applied a modified conceptual HBV model for better understanding of runoff processes in Gilgel Abay.

Of major importance for modelling the relation between rainfall and runoff is the representation of rainfall over the catchment. Whereas assessing and representing rainfall variability is of high importance, unreliable and inaccurately observed rainfall may largely impact runoff simulation results. Aspects of rainfall variability in the Upper Gilgel Abay study area are reported by Haile et al. (2009), which reveals the variability between mountainous areas and flat areas close to the lake. In Upper Gilgel Abay catchment rain measuring stations are sparse in distribution and most are located outside the catchment. Observations from rain gauge stations are available daily with some of series incomplete. Hence, Satellite rainfall products can be considered as an option for rain gauge measurements. Satellite-based rainfall estimates have become available at high resolutions and are expected to offer an alternative to represent the variability rainfall estimates in data-sparse and ungauged catchments (Sawunyama & Hughes, 2008). In this regard, different products have been produced with the development of earth observation techniques.

Rainfall variability is often influenced by nonlinear interactions between several factors like local variations of topography, the orientation of mountains and aspect (Haile et al., 2009). Terrain features also increases the variability of rainfall by means of processes such as rain shading and strong winds (Buytaert et al., 2006). Similarly, in Gilgel Abay catchment, Haile et al. (2009) revealed that the variation of rainfall is affected by topography and distance to the center of the Lake Tana. The study showed that in the basin less rainfall variation is observed over high-elevation areas than low-elevation areas. The variation in rainfall over the catchment also show temporal variability with frequent rainfall and convective activity mostly in the afternoon over the southern mountains and in the night over the southern part of the Lake Tana shore (Haile et al., 2009). Hence, in mountainous areas with a limited rain gauge network, as in the Gilgel Abay catchment, satellite-based rainfall estimation might provide information on rainfall occurrence, amount, and distribution at the highest spatial and temporal resolution (Anagnostou et al., 2010).

On the other hand, land cover changes also affect the hydrology of a catchment by modifying evaporation and thereby influencing runoff generation (Cao et al., 2009). Here, some studies (e.g. Rientjes

et al. 2011; Gumindoga et al. 2015) in Upper Gilgel Abay catchment focused on the impact of changes in land cover on stream flow and indicated the expansion of agricultural land and reduction of forest cover over the catchment (Li et al., 2012).

Furthermore, the increasing demands of water resources and intensified land cover change calls for applying physically based distributed hydrological models which are capable of modeling the spatial and temporal dynamics of runoff behavior in catchments like Upper Gilgel Abay following the rainfall patterns. Therefore, there is a need to model the spatial and temporal variability of runoff in the catchment with satellite rainfall estimates (SRE) as a major input.

1.2. Problem Statement

Rainfall-Runoff models are tools to represent and predict catchment processes. For runoff modeling, representing rainfall over time and space accurately is vital as it is one of the main causes for runoff generation. In Upper Gilgel Abay catchment rainfall stations are scarce and most are situated outside the catchment. Fortunately, with the development of earth observation technologies it is possible to use satellite rainfall estimates as forcing for hydrological modeling. As reported by scientific community, satellite rainfall estimates are contaminated with systematic errors also called bias both in temporal and spatial dimension. Hence, satellite products need to be bias corrected and their performance in representing rainfall should be evaluated before using such information for modeling work. Hence, the performance of bias corrected satellite products must be tested as forcing to simulate the runoff over long time series to have reasonable evaluation. Likewise runoff source areas (saturation excess) can be identified in response to rainfall variation over time and space for upper Gilgel Abay catchment. Assessing the dynamics of runoff behavior within the catchment by spatially distributed satellite rainfall forcing over space and time is a research gap identified and is one of the follow-up efforts of understanding the hydrology of the Upper Gilgel Abay catchment. The scientific problem here is the use of bias corrected satellite rainfall estimates which is available at high temporal (1-hr) and spatial (8 km × 8 km) resolution to be tested as forcing for the stream flow modeling in Upper Gilgel Abay catchment.

1.3. Main objective

The main objective of this study is to test the effectiveness of bias corrected satellite rainfall estimates at high spatial and temporal resolutions for simulating spatial dynamics of runoff in Upper Gilgel Abay catchment.

1.3.1. Specific objectives

- To use bias corrected satellite rainfall estimates as forcing for the REW approach in Upper Gilgel Abay catchment.
- To evaluate to what extent model performance is affected when satellite rainfall estimates are used instead of rainfall estimates from rain gauges.
- To evaluate if major runoff source areas in the Upper Gilgel Abay catchment can be identified using REW approach.
- To simulate runoff with hourly satellite-based rainfall and to evaluate how the diurnal rainfall cycle affects the stream flow hydrograph.

1.3.2. Research questions

- How accurate do satellite rainfall estimates represent rainfall for the modelling of runoff in Upper Gilgel Abay catchment?
- Where are the major runoff source areas located in the Upper Gilgel Abay catchment?
- Can locations of these areas be related to rainfall distribution?
- How does the stream flow hydrograph change when hourly satellite-based rainfall data is used instead of data at the daily time step?

1.4 Relevance of the study

This study is to evaluate if the REW with rainfall inputs from high spatial and temporal resolution satellite products can serve to better understand the dynamics of runoff behavior and runoff generation in Upper Gilgel Abay catchment. This modeling effort is a test case for the use of Satellite rainfall estimates (SREs) for modelling runoff source areas at sub-daily time scales. Such modelling is not demonstrated for the Gilgel Abay basin in Ethiopia.

1.5 Thesis outline

The thesis has six chapters which include introduction, study area and data availability, literature review and model description, methodology, result and discussion and conclusion and recommendation.

The Introduction chapter deals with a general background related to the study theme, justification and objectives for conducting this work. The relevance of the study is described in this chapter as well. The second chapter is about the description of the study area and the nature and quality of data. Descriptions are added on the collected data during a field work period and the satellite images that were used to achieve the objectives of the study.

In the third chapter (literature review), related researches conducted in the study area and theme were reviewed. The fourth chapter describes the scientific methods which were applied for processing the data, model simulation procedures, analysis conducted, and the REW model and balance equations. Results and discussion, which addresses answers for the research questions, are presented in the fifth chapter. The final or sixth chapter forwards the conclusion and recommendations of the thesis work.

2. STUDY AREA AND DATA AVAILABILITY

2.1. Study area description

2.1.1. Geographical location and topography

Upper Gilgel Abay catchment is located in north-western Ethiopia with geographical coordinates of 10°56' to 11°51'N latitude and 36°44' to 37°23' E longitude. The catchment represents the gauged part of Gilgel Abay river basin. The total area of Upper Gilgel Abay catchment is 1657km². The river originates in a place known as Gish Abay which is near a small town Sekela and it is the largest contributor to the inflow of Lake Tana (Rientjes et al., 2011). As shown in figure 2, the topography of catchment is characterized as rugged with highest elevation around 3504 meters and lowest around 1892 meters. Based on the information from SRTM Digital Elevation Map of the catchment, the south and south eastern part of the catchment is highland where mountain ranges are found and the Northern part of the catchment is characterized by relatively flat terrain.

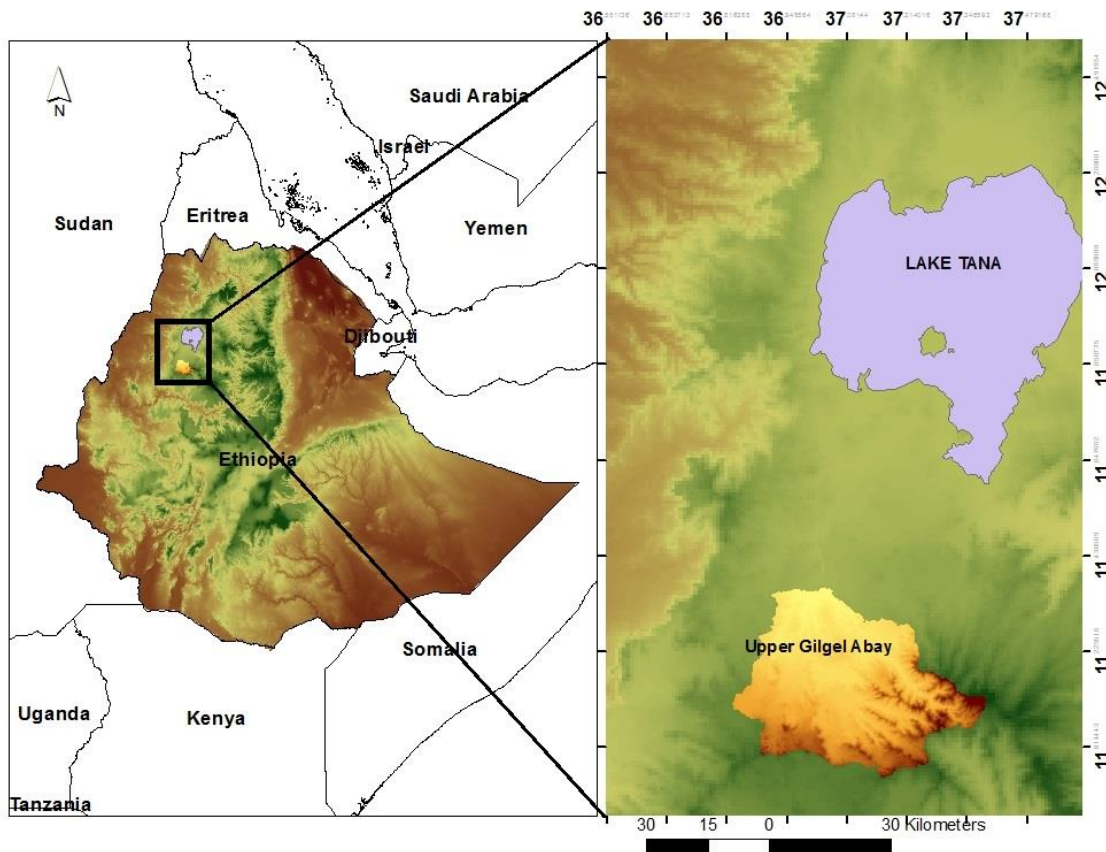


Figure 1: Location of Upper Gilgel Abay catchment

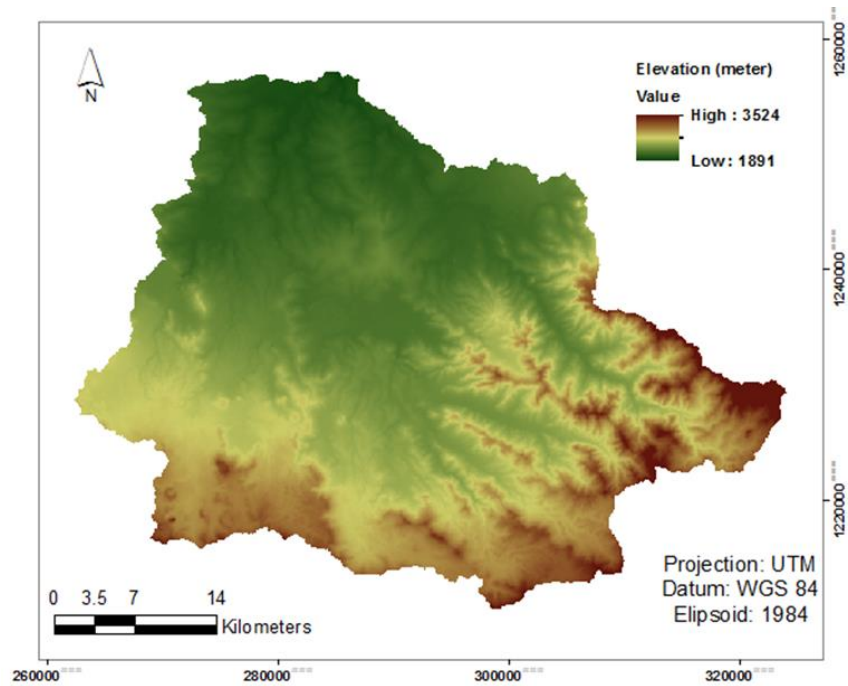


Figure 2: Elevation map of Upper Gilgel Abay catchment

2.1.2. Climate

The climate of Upper Gilgel Abay is dominated by the tropical highland monsoon. The main rainy season is from June to September during which south-west winds bring rains from the Atlantic Ocean. Some 70-90 percent of mean annual rainfall occurs during this season (Taddele, 2009). As depicted in figure 3, the dry season starts in October and last till January with a short rainy period from February to May. In figure 3 average daily rainfall of the catchment is plotted and indicates the rainy seasons with their specific characteristics.

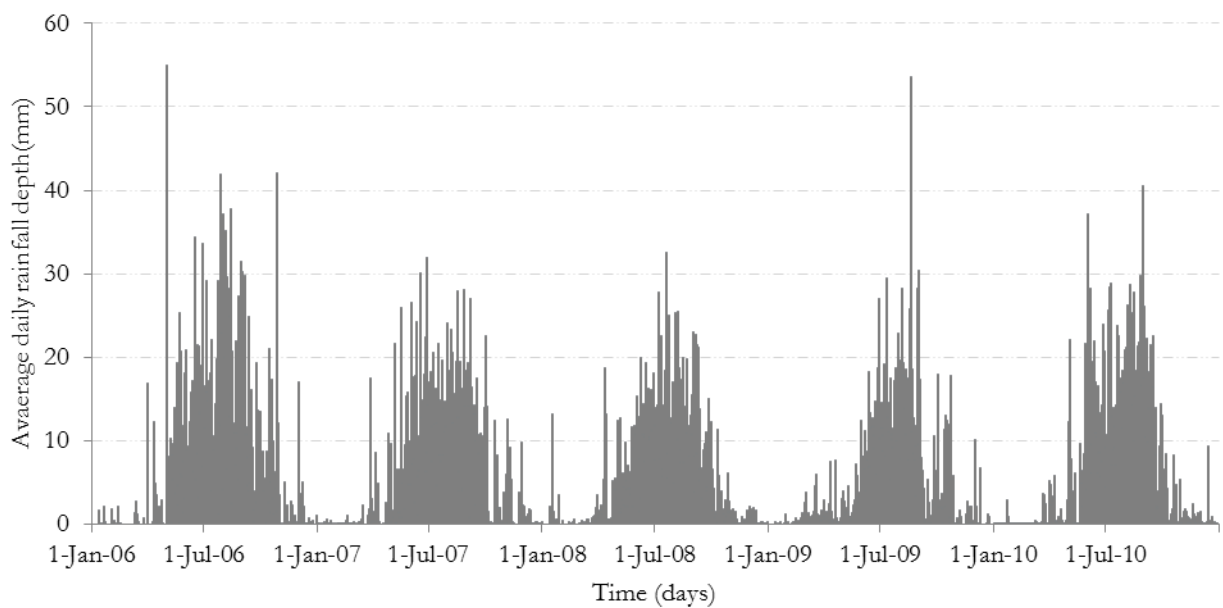


Figure 3: Basin averaged daily rainfall of Upper Gilgel Abay catchment (2006-2010)

In the period of 2006 to 2010, the average daily rainfall of the catchment which is weighted using Thiessen polygons indicates clear spatial and temporal variability of rainfall. There is a decreasing trend of rainfall from south to north following topography. Average temperature measured in gauging stations (see Table 1) for 2006-2010 period shows small variation (see figure 4). The diurnal range of temperature on average varies between 15 to 23 °C.

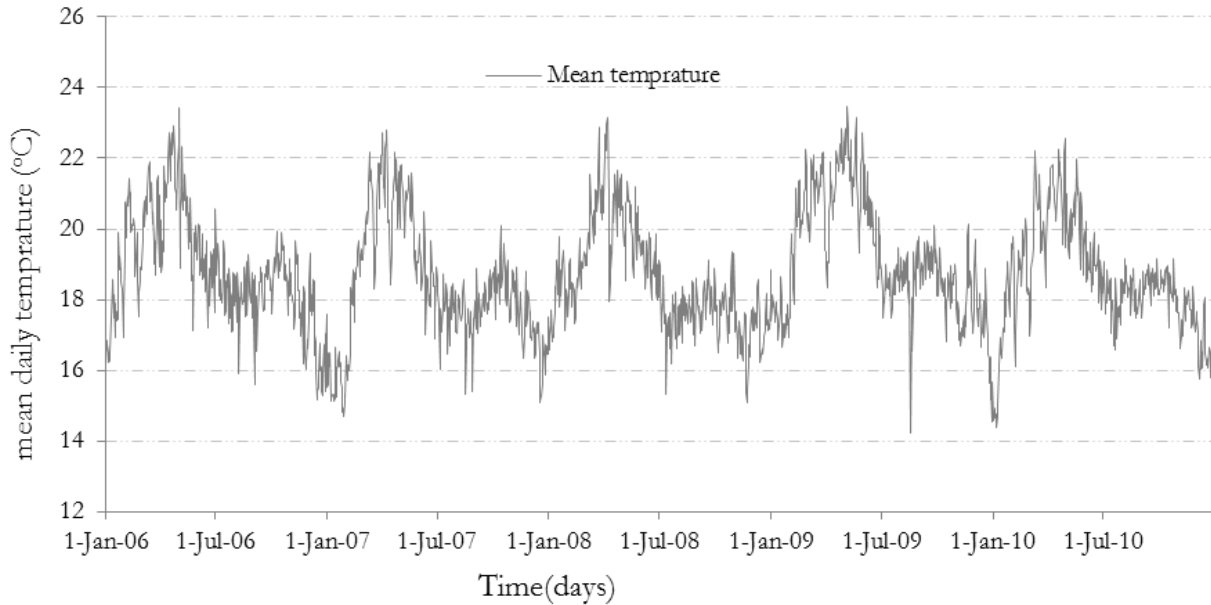


Figure 4: Average daily temperature of Upper Gilgel Abay catchment (2006-2010)

2.1.3. Land use/Land cover, Soil and Geology

Most of the Upper Gilgel Abay catchment area is dominated by cropland with some woodlands and forested highlands. Besides the cultivated lands, the main land cover types are grassland, marshland, and forest with frequent patches of shrubs, eucalyptus woods and trees (Gumindoga et al., 2015). Land cover change studies in the Upper Gilgel Abay catchment show that forest land decreased from 50.9% in 1973 to 32.9% in 1986 (see Rientjes et al., 2011) . Agricultural land increased from 28.2% in 1973 to 40.2% in 1986. Forest on the other hand, decreased from 32.9% to 16.7% while agricultural land increased from 40.2% to 62.7 % for the 1986-2001 period (Rientjes et al., 2011).

Soils are characterized by clay, clay loam and silt loam textures, each texture sharing similar proportions of the catchment area (Bitew & Gebremichael, 2011).The geology is characterized by scoraceous and fractured quaternary basalts underlying most part of the Upper Gilgel Abay catchment that show the highest groundwater potential as indicated by its high infiltration capacity and hydraulic properties. Many high discharging springs emerged from this rock unit and acts as the base flow for Gilgel Abay River, which drains to Lake Tana. Alluvial sediments are also found along the mouth of the Gilgel Abay river (after Kebede, 2013).

2.2. Data Availability

2.2.1. Insitu measurement

2.2.1.1. Meteorological Variables

In the area inside and outside of the study catchment meteorological stations of different level are found (see figure 5) and collected from Regional Meteorological office in Bahir Dar. Based on the classification of the office there are principal, also termed level one stations, where precipitation, air temperature, wind speed, relative humidity and sunshine duration measurements are taken every three hours. Another set of stations are class three stations (ordinary), where precipitation and air temperature measurements are taken daily. In addition class four stations only serve for precipitation measurements at daily base. Based on this classification Adet, Dangila and Bahir dar are principal stations. Class three stations are Kidamaja and Wetet abay and class four stations includes Enjibara and Sekela.

Table 1: Shows meteorological variables collected for this study

Met. stations	longitude	latitude	Elevation	Rainfall	Temperature (max, min)	Relative humidity	Sunshine duration	Wind speed
Adet	332663.3	1245939.5	2180	x	x	x	x	x
Bahir dar	324455	1281713	1797	x	x	x	x	x
Dangila	262994.7	1244290.6	2119	x	x	x	x	x
Sekella	304679.7	1214109.7	2690	x	x			
Enjibara	270514	1213131	2540	x	x			
Kidamaja	259513	1216653	1913	x	x			
Wetet	287108.5	1257029.5	1920	x	x			

“x” in the table indicates meteorological variables that were collected during fieldwork.

As shown in table 1, measurement variables, geographic coordinates and elevation of seven meteorological stations selected for this study are shown. Measurement time series cover the period of 2006-2010. As shown in figure 5, most of the meteorological stations are outside the catchment. The gauging station where discharge measurements are taken is located in the Northern tip of the catchment.

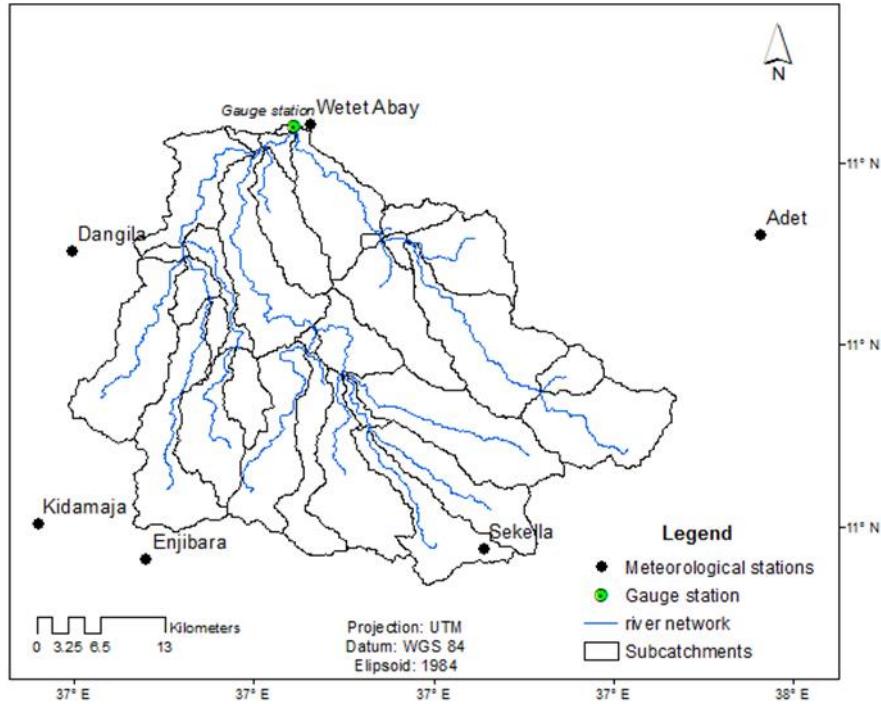


Figure 5: Location of meteorological and gauging stations considered in Upper Gilgel Abay catchment

After filling-in observed gaps in observation time series, annual rainfall of each meteorological station is calculated and shown in figure 6. Enjibara, Kidamaja and Sekela are stations which receive more than 2000 mm per annum. These stations are located in high altitude areas. The inter-annual distribution of rainfall in the study area is mainly affected by the location of the Intertropical Convergence Zone (ITCZ) which is caused by a low-level wind convergence (Haile et al., 2011). Adet, Dangila and Bahir Dar stations which are located in low laying areas of the catchment show lower annual rainfall (less than 2000 mm) per annum.

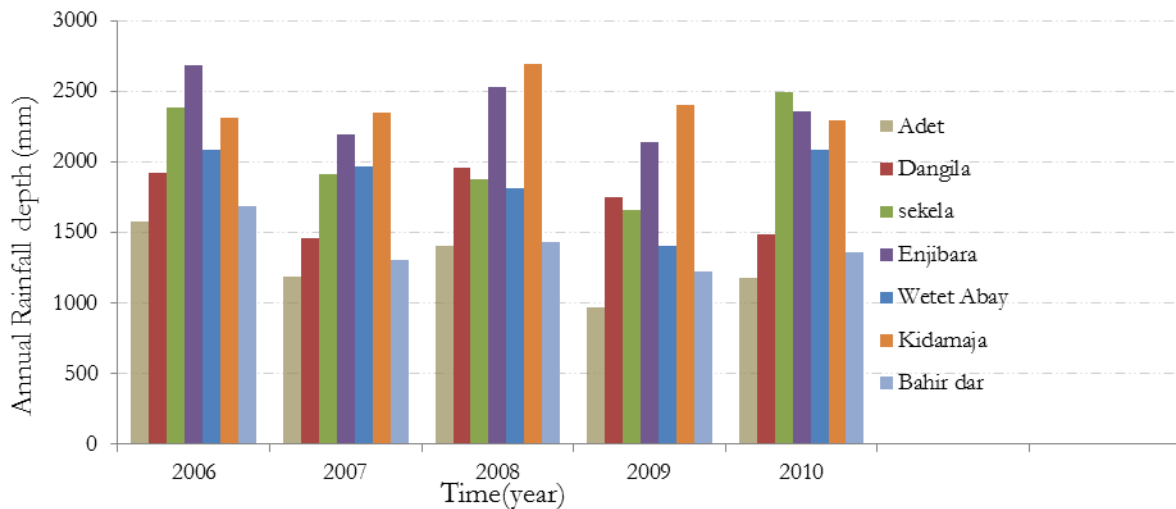


Figure 6: Annual rainfall of Upper Gilgel Abay catchment for meteorological stations

2.2.1.2. Hydrological Data

Discharge data by means of a stage-discharge relation is manually measured at daily base at the outlet of the catchment (near Bicolo Abay town). During field visit, observation time series were collected from the

Ministry of water and energy for a period of 5 years (2006-2010) as shown in figure 7. Screening was done for the extreme outliers (for instance in the case of July 2008 which is shown in figure 7) and missing dates with reference to the historical discharge measurement (1974-2005).

As shown in figure 7, there are missing values in the year 2006 and a sharp drop in discharge in 2008.

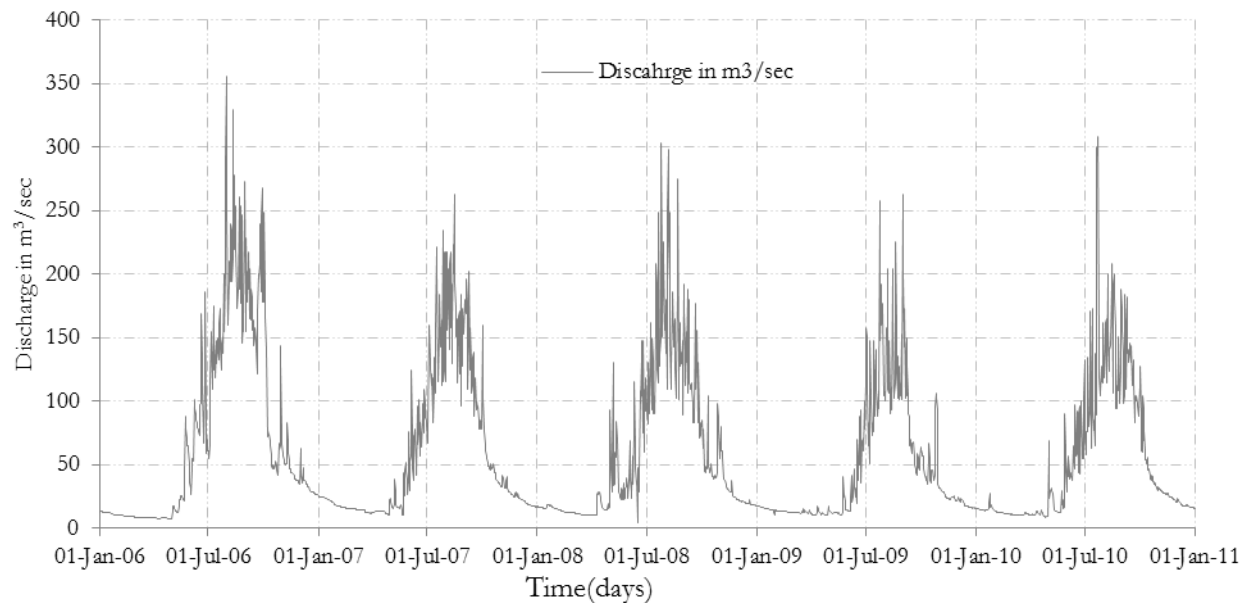


Figure 7: Discharge measurement taken in the outlet of Upper Gilgel Abay catchment

2.2.2. Remote sensing data

Satellite based data products collected and used for this study are a Digital elevation model (DEM) and CMORPH (Climate Prediction center Morphing technique rainfall products).

Digital elevation model is available by NASA Shuttle Radar Topographic Mission (SRTM) with a spatial resolution of 3 arc second (approximately 90 meters). The data is available freely and downloaded from the USGS SRTM website (<http://srtm.csi.cgiar.org/>).

Satellite rainfall estimate of CMORPH product was downloaded for 5 year period (2006-2010) through ISOD extension of Ilwis software having 1-hour temporal resolution and 0.07277 degrees (approximately 8 km) spatial resolution. CMORPH estimates are derived from the passive microwaves aboard the DMSP 13, 14 & 15 (SSM/I), the NOAA-15, 16, 17 & 18 (AMSU-B), and AMSR-E and TMI aboard NASA's Aqua and TRMM spacecraft, respectively (Joyce et al., 2004).

3. LITERATURE REVIEW

3.1. Sattelite rainfall estimates as forcing for Modeling runoff

Rainfall-runoff simulation is mainly dependent on how well spatiotemporal variability of rainfall fluxes are represented (Hong et al., 2007). Satellite-based rainfall estimates have become available at high temporal and spatial resolutions and are expected to offer an alternative to represent the variability rainfall estimates in data-sparse and ungauged catchments (Sawunyama & Hughes, 2008). In this regard, different products have been produced with the development of earth observation techniques. One of the products that is available at a global scale with high spatial ($8 \text{ km} \times 8 \text{ km}$) and temporal (30min.) resolution is CMORPH.

The accuracy of the 1-hr, $8 \text{ km} \times 8 \text{ km}$ CMORPH product for a Lake Tana basin, which is characterized by large topographic variability and significant rainfall variation, is shown by Haile et al. (2013). Findings show the poor rain detection capability of CMORPH which led to significant underestimation of the seasonal rainfall depth with large amounts of hit rain bias as well as missed rain and false rain biases. The findings also indicated the effect of the spatial differences in highlands and lowlands in rain event properties which are reflected on spatial differences in CMORPH accuracy (Haile et al., 2013). Hence, reducing the bias of the product 1-hr, $8 \text{ km} \times 8 \text{ km}$ CMORPH which is used in this study is an important procedure before using as input for modeling the spatial dynamics of runoff.

Satellite rainfall estimates often do not match with rain gauge measurements. Differences are considered as errors that can be caused by: (1) Satellite rainfall estimates are indirect estimates of rainfall from cloud properties observed from space in case of Geo-stationary satellites and derived from microwave emissions from rain drops and scattering from ice in orbiting satellites (Qin et al., 2014). (2) Assumptions like the surface emissivity, neglecting evaporation below clouds, and empirical relationships are the driving factors of error (Alemohammad et al., 2015) (3) Satellite rainfall estimates errors are caused by various factors like sampling frequency, field of view of the sensors, and uncertainties in the rainfall retrieval algorithms (Nair et al., 2009).

Errors as such can be random or systematic. It is the Systematic error that is commonly referred to as bias and reflects errors which are systematically distributed over time and space. Bias in satellite rainfall products can cause large uncertainties in hydrologic modeling (Habib et al., 2014). Different bias correction algorithms are proposed in research to minimize the systematic error which exists in satellite rainfall estimates. In Lake Tana basin specifically, Habib et al. (2014) applied three bias correction schemes which are Space-time fixed, time variable and space-time variable bias factors to correct the bias of CMORPH and found the bias which needs most important correction is the temporal variation of CMORPH. Details of bias correction algorithm applied in this study are found in section 4.4 page 18.

Some studies report on Stream flow simulations based on SREs forcing. Bitew et al. (2012) evaluated the performance of high-resolutions ($0.25^\circ \times 0.25^\circ$ spatial and 3 hr. temporal) satellite rainfall products (CMORPH, TMPA 3B42RT, TMPA 3B42, and PERSIANN) as input for stream flow simulation in mountainous watershed in Ethiopia and found CMORPH and 3B42RT had smaller biases compared to PERSIANN and 3B42. Haile et al, (2012) also reported CMORPH ($8 \text{ km} \times 8 \text{ km}$ spatial and 3 hr. temporal resolutions) as a better product than TRMM-3B42 RT and TRMM-3B42 PRT (which both have $0.25^\circ \times 0.25^\circ$ spatial and 3 hr. temporal resolutions) in capturing the diurnal cycle of rain rate in Lake Tana basin. They also indicated the necessity of correcting satellite products before using as input to hydrologic models.

3.2. Runoff processes

One of the important questions in hydrology is how much discharge occurs in a river in response to a given amount of rainfall. To answer this question we need to know how much it rains, where it rains, where and how water is stored in the different land surface zones and what pathways water follow to reach the stream channel. These are some of the questions which can be addressed in rainfall – runoff studies. The term Runoff is used for Overland flow and shallower interflow processes and groundwater that transport water to the river approximately a day. The component of groundwater (base flow in streams and rivers) moves at much lower velocities and reaches the stream over longer periods of time such as weeks, months or even years (Tarboton, 2003).

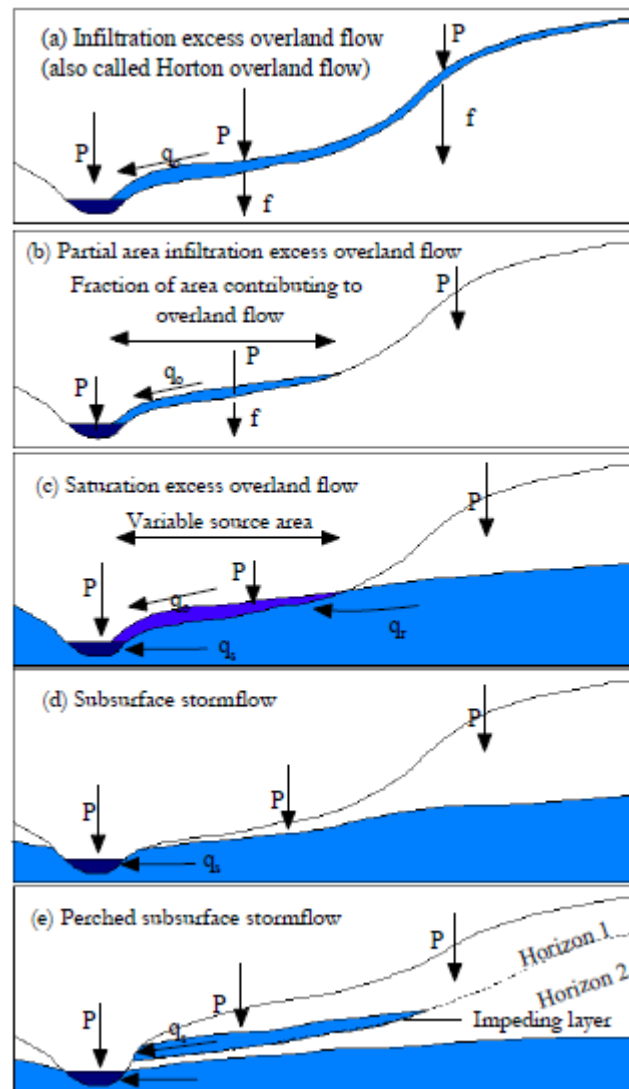


Figure 8: classification of runoff generation mechanisms (Source: Tarboton (2003) adapted from (Beven, 2000)).

The main hydrological mechanisms that generate overland flow are infiltration excess and saturation excess. Infiltration excess is generated when rainfall intensity exceeds the infiltration capacity of the soil causing overland flow to generate (see fig.8a) (after Beven, 2012). It is based on the concept that runoff is generated when rainfall rates exceed soil infiltration capacity so runoff amount is directly controlled by factors that determine soil infiltration capacity, such as land use, soil type and moisture content (Lyon et al., 2006). Infiltration excess overland flow is commonly referred to as Hortonian overland flow.

Saturation excess is fundamentally different since overland flow is not generated by high rainfall intensities but by land surface saturation as a result of soil saturation by a rising water table. Saturation zones occur close to river reaches at lower lying areas in a basin that are characterized by exfiltration zones (see fig.8b). Unlike Hortonian flow, where soil type and land use basically play a controlling role in runoff generation, landscape position, local topography, and soil depth are some of the major factors controls on saturation excess runoff that varies for different catchment. Saturation excess is at the base of the Variable Source Area(VSAs) concept (Tarboton, 2003) that acknowledges that the spatial extent of saturation excess varies seasonally, depending on the relative rates of rainfall and evapotranspiration (Walter et al., 2004).

Variable source areas are generating runoff of type saturation excess from shallow ground water flowing into the soil from upslope areas of the watershed. They become active when groundwater flow exceeds storage or when precipitation falls on the saturated area, causing saturation excess runoff (Easton et al., 2008). In most watersheds, both Hortonian and saturation excess processes contribute to runoff generation; however, one or the other often dominates (Walter et al., 2004).



Figure 9: Typical surface with saturation excess (exfiltration) in the Upper Gilgel Abay catchment (photo: Dr.Ing. T.H.M. Rientjes).

Topography is a key landscape component that needs to be considered in understanding the runoff processes of Upper Blue Nile Basin and specifically Upper Gilgel Abay catchment where runoff in the basin is generated both as saturation excess and infiltration excess runoff mechanisms (Dessie et al., 2014). Figure 9 is one of the typical saturation excess mechanisms generated when the water table dissects the land surface. The photo was taken in the Gilgel Abbey catchment near Sekela at the end of wet season (Courtesy Dr.Ing. T.H.M. Rientjes). Gilgel Abay catchment has high infiltration capacity up to 20% and overlaid by dominantly scoraceous and fractured quaternary basalts (Kebede, 2013).

Another runoff generation mechanism is subsurface flow or interflow shown in fig 8d and e. Subsurface flow is generated by rapid infiltration of rain and the associated increase in soil hydraulic conductivity. Infiltrated rainfall may flow rapidly through the soil mantle more or less directly to the stream via interconnected large pores or porous structural features (macropores), or through saturated horizons at the base of the soil mantle or perched at permeability contrasts within the soil mantle. If rapid flow through the soil occurs, current storm rainwater dominates the storm runoff. Central to all the mechanisms discussed is the concept of runoff contributing zones which expand and contract seasonally and during storms, depending on antecedent wetness, soil physical properties, water table elevations, and storm magnitude (Pearce et al., 1986).

3.3. Hydrograph components

A stream flow hydrograph has different components or sections that are visually taken as reference for a hydrologist in understanding the hydrologic regime of a catchment. Among different components peak, lag time, base flow, storm flow, rising limb, recession limb are most commonly used in hydrograph reading (see figure 10). In this work, peak flows (high flows) are the portion of stream flow which normally seen as the highest discharge events in a hydrograph and that can be caused by high-intensity precipitation (Davie, 2008). Definitions of other components can be found in any hydrology book.

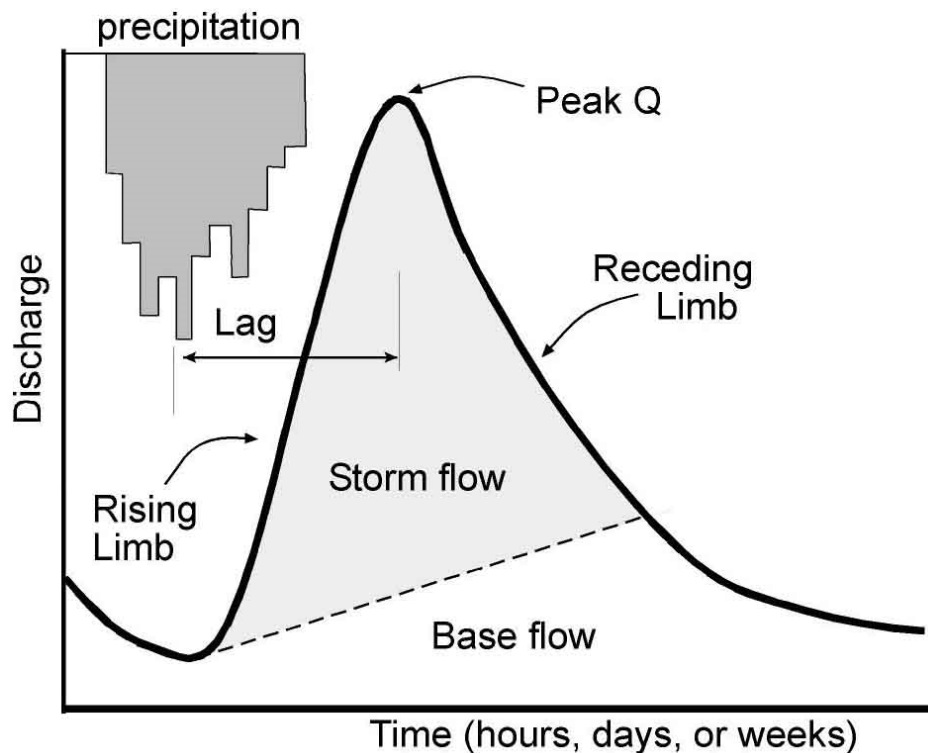


Figure 10: stream flow hydrograph (from public resource GeogOnline)

<https://snowhydro1.wordpress.com/2012/04/13/l-is-for-lag-time/>

4. METHODOLOGY

4.1. Methodological approach

To achieve the objectives of this study hydro-meteorological and SREs data are collected. The missing values in hydro-meteorological data were filled-in with climatological mean and regression analysis techniques. The satellite product (CMORPH and SRTM DEM) also were processed in steps like extraction and bias correction schemes before using the data as input for REW. Model configuration, code testing, model initialization, simulation, calibration and validation are procedures applied in modelling. The flowchart in Figure 11 summarizes the steps used in this study that is further described below.

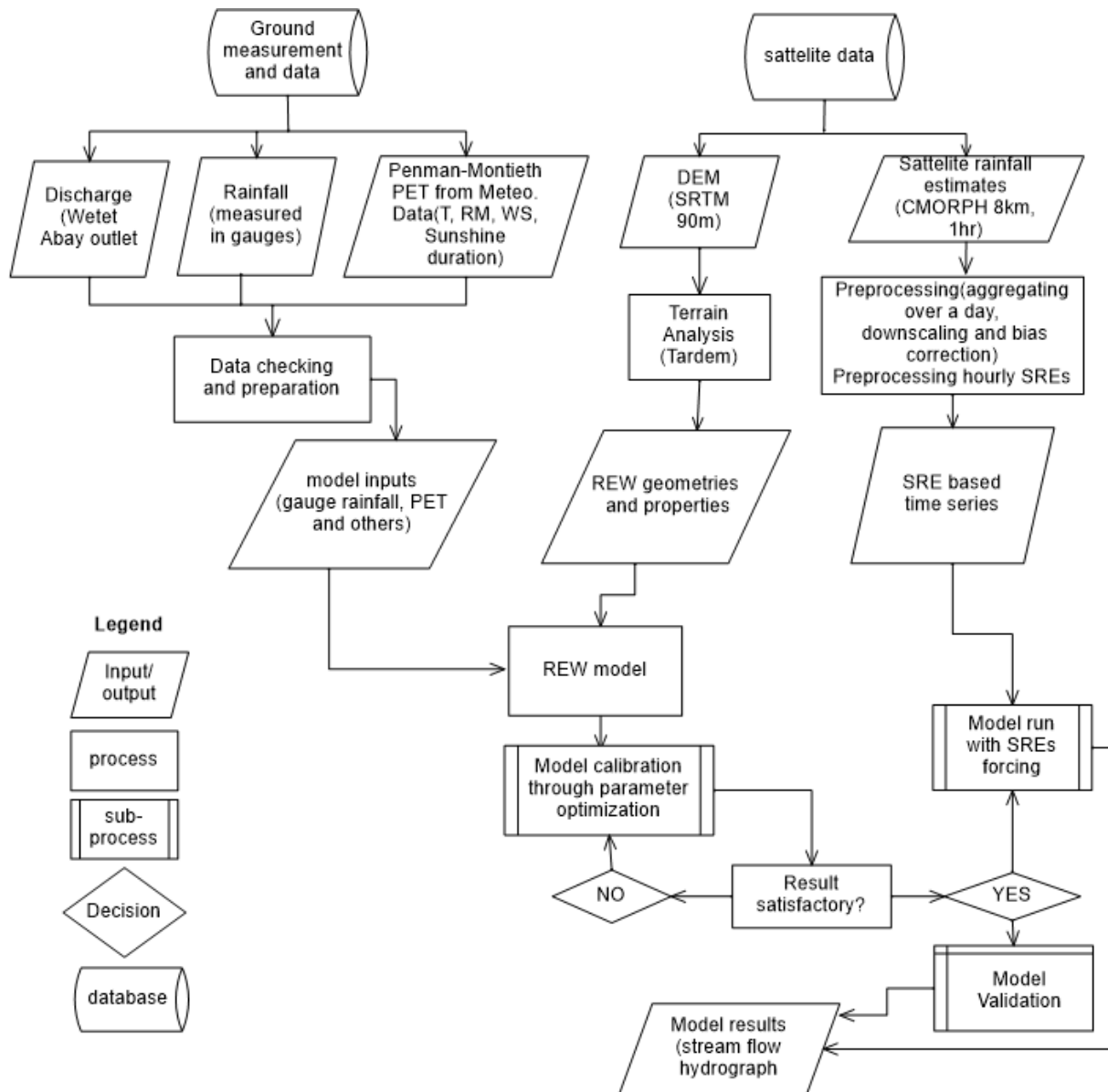


Figure 11: Flowchart showing the procedures and methods

4.2. Processing satellite rainfall estimates

The CMORPH (1-hr, temporal and 8 km × 8 km spatial resolution) product is chosen for this study for representing rainfall distribution over the Upper Gilgel Abay catchment. CMORPH produces global precipitation estimates at high spatial and temporal resolution. CMORPH uses half-hourly interval geostationary satellite Infrared imagery to propagate the relatively high-quality precipitation estimates derived from passive microwave data (Joyce et al., 2004). The product can provide rainfall estimates at hourly time step which is finer than gauge measurement frequencies (daily) and for 8 km × 8 km grid element.

The procedure that was used to prepare the satellite rainfall estimates for model input is the following:

4.2.1. Extraction of SREs

A point map showing the location of rain gauging stations were created for the meteorological stations which measure rainfall daily. The CMORPH Version 1 (1-hr, temporal and 8 km × 8 km spatial resolution) product was selected and downloaded for the period 2006-2010 through the ISOD toolbox of Ilwis. With the aid of *maplist* and Ilwis script, SREs for pixels where rain gauging locations fall was extracted for comparing with surface based rain gauge measurements.

4.2.2. Bias correction scheme

Scatterplot graphs and statistical indices like mean, standard deviation and coefficient of variation were used for evaluating the performance of CMORPH against gauge measurements. This helps to get an overall impression of the performance of CMORPH in the study period and site. The correction factors have been applied for correcting systematic errors of satellite rainfall estimates of CMORPH. The total bias is estimated in the formula below.

$$\text{Total bias} = \sum_{i=1}^n R_S - \sum_{i=1}^n R_G$$

Where R_S and R_G represents CMORPH and gauge rainfall estimates respectively.

The bias correction scheme that was applied to correct satellite rainfall estimates is Time and space variant because it enables to apply correction over time and space depending on the variability of rainfall estimate and is adapted from Habib et al. (2014). The algorithm was applied in Upper Gilgel Abay catchment and performs better than time-invariant, and time-variant and spatially invariant correction schemes.

For a selected day (d) and gauge (i), the multiplicative daily bias factor (BF) at a certain CMORPH pixel with a collocated gauge can be formulated as follows.

$$BF_{TVS} = \frac{\sum_{t=d}^{t=d-L} S_{(i,t)}}{\sum_{t=d}^{t=d-L} G_{(i,t)}}$$

Where G and S represent daily gauge and CMORPH rainfall estimates, respectively, i refers to gauge location, t refers to a Julian day number; and L is the length of a time window for bias calculation. The time window used for this study is selected as 7 days with minimum 5mm gauge rainfall accumulation based on preliminary analysis of the dataset and previous studies in the area by Habib et al. (2014). If the rainfall accumulation is less than 5mm, no bias correction was applied to that specific time window.

Measurements from gauging stations (point) were compared to pixel values (size 8km × 8km), which indicates that the correction scheme ignores the possible error that can be produced by point to area

comparison. However, the spatial correlation assessment of point-grid element in the study catchment indicates 0.91 for seven-day accumulation period, which can be taken as reasonable to use point to pixel comparison for seven-day time window (Habib et al., 2014).

For getting bias correction factors (BFs) point to pixel comparison has been used. After getting BFs for seven day time window and for each rain gauging stations the respective point maps were created. The point maps were interpolated with Inverse distance technique and used to correct the respective CMORPH maps (see Appendix IV). Having bias corrected CMORPH rainfall image over the Upper Gilgel Abay catchment allows to overly with the raster map showing the REWs. After overlay average areal weighted SREs for each REW were aggregated. The REW averaged satellite rainfall estimates then used as forcing for respective REW centroids. With this procedure bias corrected SREs for each time step and REW area was obtained. The approach has enabled to use the centroids of each REW as station location, and to take as locations of rainfall estimates. Hence, REW averaged SREs and finer time step than daily was used for preparing SRE based time series. The approach has an advantage of extracting the spatial information which is available in Satellite rainfall estimates to better represent the spatial-temporal variability within the catchment.

4.3. Comparison of stream flow simulation using rainfall forcing of daily and hourly CMORPH

In the study catchment, water level measurements (i.e. river stages) are taken each day at 8 a.m. at Bicolo Abay town. By means of a stage-discharge relation, stage measurements are converted into daily discharges. When considering that temporal variability of rainfall in terms of intensity and depth directly affects runoff production, high flows, low flows, lag time and time to peak. The use of high-resolution satellite product which is available at hourly time step would allow representing the diurnal rainfall distribution and intensity.

Hourly estimate is used as input for simulation of discharge at hourly time step. 3 rainy months (June, July and August) of the year 2010 were selected for hourly time step based streamflow simulation. The bias factors, methods employed for extraction of SREs, analysis were similar to the daily time step CMORPH. (see section 4.2). To reduce the impact of initial condition the model run up to May 31, 2010 as warming up period. Visual inspection and objective function of RVE were used for evaluation of the model results.

Exceedance probability which defines the percentage of time that discharge can be equaled or exceeded (P) is used for comparing hourly and daily CMORPH based stream flow simulation.

$$p = 100 * \left(\frac{M}{(n+1)} \right)$$

Where, M the ranked position on the list which is dimensionless and n is the number of events for the period of record which is also dimensionless (<http://water.oregonstate.edu/streamflow/>).

4.4. Filling in techniques used for missing gauge measurements

Climatological mean of the day (CMD):

This method uses the long-term average value of the same day of interest (Narapusetty et al., 2009). In this approach, a missing value will be filled by taking the long-term mean of the same calendar day. This method considers the same day will have the probability to have a similar meteorological value with the observed data of same day for all year (Narapusetty et al., 2009). The approach is similar to the mean substitution method of Kotsiantis (2006) and was used to fill missing values in the study.

Regression analysis:

In multiple linear regression, a linear combination of two or more predictor variables can be used to explain the variation in a response (Abatzoglou et al., 2009). Regression analysis was applied to fill in incomplete rain gauge records in Sekela Station as the missed records were in rainy months. The rainfall records of other stations (Adet, Dangila, Enjibara, Kidamaja and Wetet Abay) were used as predictors in the regression analysis.

4.5. Penman-Monteith equation for Potential Evaporation

Several algorithms have been developed to estimate potential evapotranspiration from climatological and field measurements. Each algorithm has different calculation and performances for different locations. The FAO Penman-Monteith method is mostly used in all regions and climates and is a standard method for estimation of the reference evapotranspiration (ET_0) (Allen, 1998). Climatological parameters of sunshine, maximum and minimum temperature, humidity and wind speed are inputs needed to calculate evaporation from open water surface and a hypothetical grass reference crop with an assumed crop height of 0.12 m, a fixed surface resistance of 70 s m^{-1} and an albedo of 0.23 (see figure 12) (Allen, 1998).

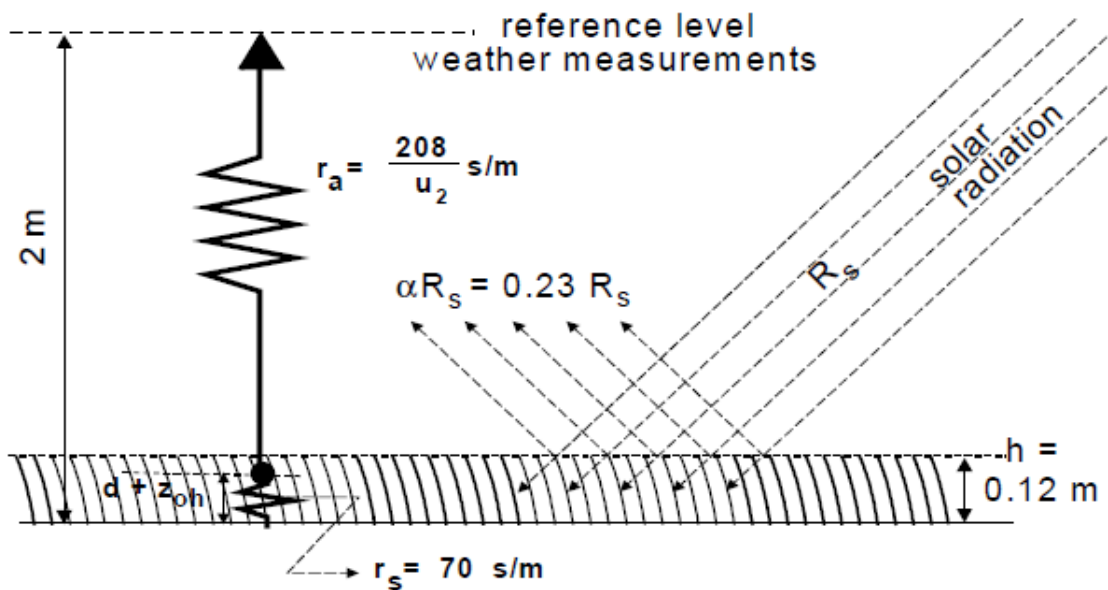


Figure 12: Characteristics of the hypothetical reference crop (Source: (Allen, 1998))

The FAO Penman-Monteith which is derived from the Penman-Monteith and the equations of the aerodynamic and surface resistance depicted below (Allen, 1998):

$$ET_0 = \frac{0.408\Delta(R_n - G) + \gamma \frac{900}{T + 273} u_2 e_s - e_a}{\Delta + \gamma(1 + 0.34u_2)}$$

Where:

ET_0 , Reference evapotranspiration [mm day^{-1}];

R_n , Net radiation at the crop surface [$\text{MJ m}^{-2} \text{ day}^{-1}$];

G , Soil heat flux density [M] $m^{-2} day^{-1}$];

T , Mean daily air temperature at 2 m height [$^{\circ}C$];

U_2 , Wind speed at 2 m height [$m s^{-1}$];

e_s , Saturation vapour pressure [kPa];

e_a , Actual vapour pressure [kPa];

$(e_s - e_a)$ Saturation vapour pressure deficit [kPa];

Δ , Slope vapour pressure curve [kPa $^{\circ}C^{-1}$]; γ ,

Psychrometric constant [kPa $^{\circ}C^{-1}$],

The full details of the calculation procedures are explained in (Allen, 1998, p. 66)

4.6. Digital elevation model (DEM) processing

SRTM DEM version 4 with a resolution of 90 m was used for the pre-processing of terrain information for the extraction of drainage network features as required as input by the hydrologic model. The terrain analysis software TARDEM was used for extracting the REWs and performing hydro processing. It also calculates the REW geometries, connectivities and properties (Reggiani, 2012).

According to the Strahler ordering system all exterior links have order 1, when two upstream links having the same order joint the order will increase by 1 (see figure 13), with the increases of same order links and segments of links streams will be generated (Tarboton et al., 1991). Here using different Strahler orders (the REWs delineated in the second Strahler order are shown in figure 13) has delineated different number of REWs (model domains) that can be used for simulation of runoff.

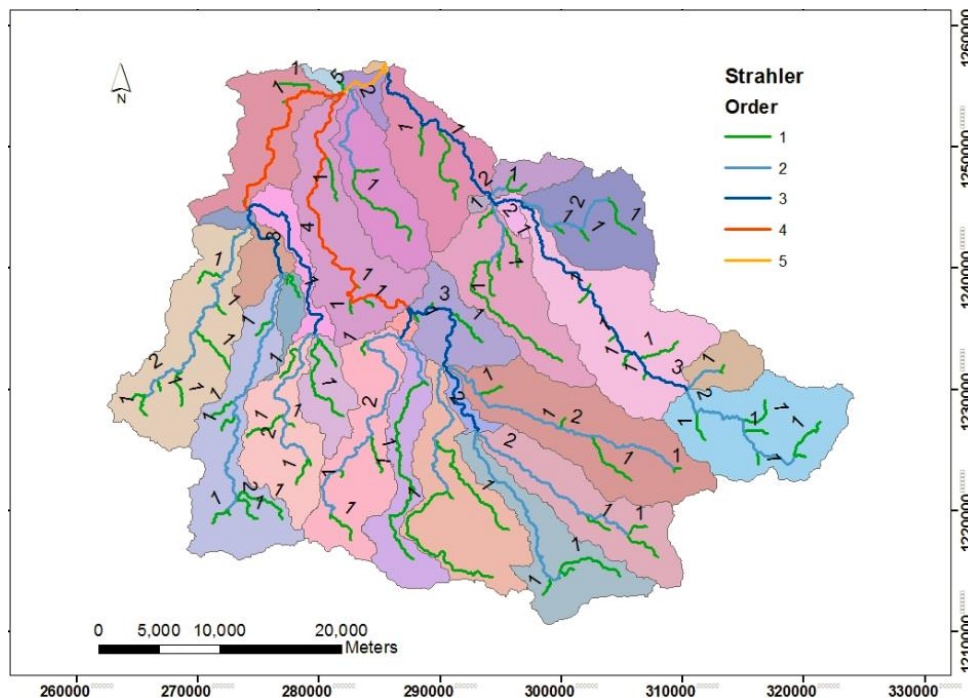


Figure 13: REWs delineated with Second Strahler order

In Upper Gilgel Abay catchment when using first and second Strahler orders, 33 and 173 subcatchments were delineated respectively as shown in Figure 14 left and right. Choice was made here to use 33 REWs as modeling domains for simulating streamflow.

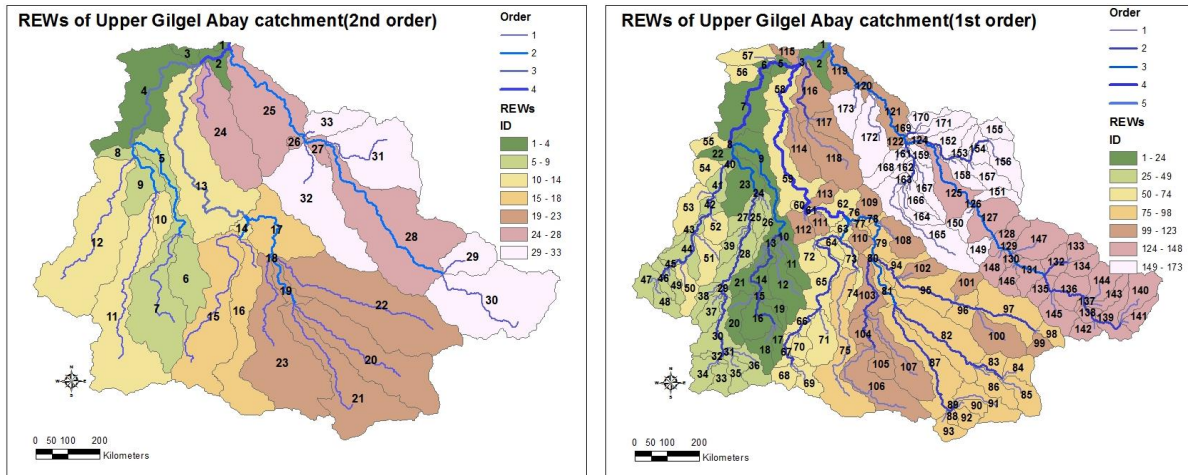


Figure 14: Discretization of the Upper Gilgel Abay river catchment into 33 REWs (Left) and 173 REWs (Right) based on Strahler order used

4.7. Model description

The model chosen is the Representative Elementary Watershed model (REW). REW is a physically based approach which is developed by Reggiani et al. (1998, 1999, 2000, 2001) and further extended with the works of Reggiani & Schellekens (2003); Reggiani & Rientjes (2005); Zhang et al. (2005). The modelling units (REW) can be hillslope or catchment shaped and linked by channel reaches that reflect the topographic structure of the catchment (Reggiani & Rientjes, 2005). REW model is an integrated hydrological simulation approach developed to simulate the entire hydrological cycle (simulates saturated, un-saturated zone, channel and overland flow zones). The approach has been developed and used for water balance studies and rainfall-runoff simulations (see Reggiani, 2012).

The REW approach has the advantages of solving balance equations of mass, momentum and energy for control volumes with in each modelling inputs (REW) for describing the hydrological processes on the catchment over other models like HBV and TOPMODEL which were applied in the study area. In the REW approach a catchment is delineated in to sub-catchments using topographic divides as shown in figure 14. Sub-catchments created are called representative elementary watersheds (REWs). These REWs are spatial entities that can be used for runoff modelling.

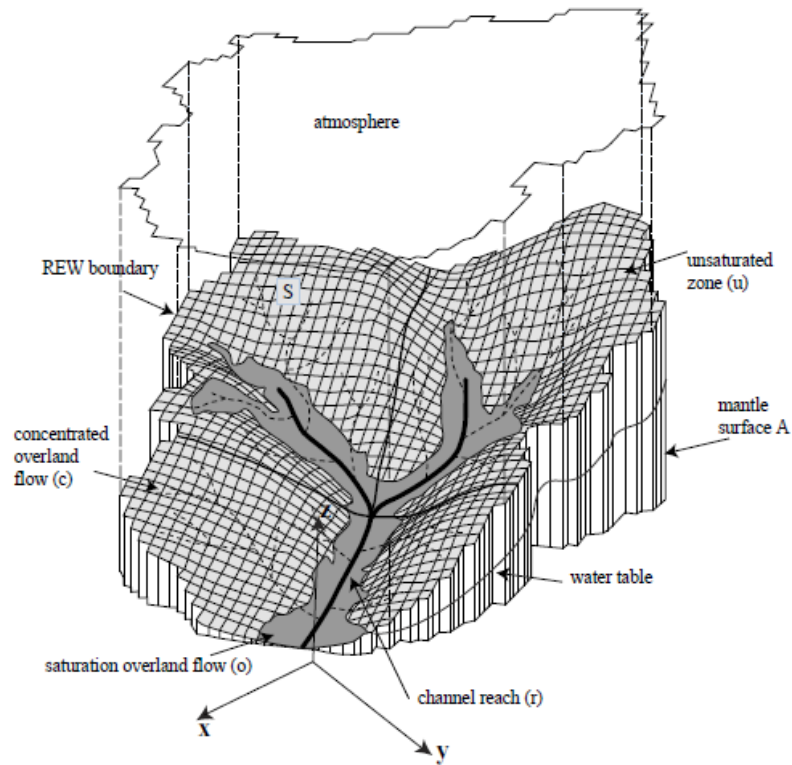


Figure 15: Three-dimensional view of REW model (Source:(Reggiani & Rientjes, 2005))

As indicated in Figure 16, “Representative elementary watersheds further have 5 zones (saturated zone (which is below the water table), unsaturated zone (above the water table), river channel, concentrated overland flow zone (soil surface corresponding to the unsaturated zone) and saturated overland flow (soil surface corresponding to the saturated zone) (Fenicia et al., 2005). The zones are symbolized as s, u, r, c, o respectively. A volume of a REW is delimited at the bottom by a horizontal impermeable surface, on top by the land surface, and laterally by a vertical prismatic mantle (Fenicia et al., 2005).”

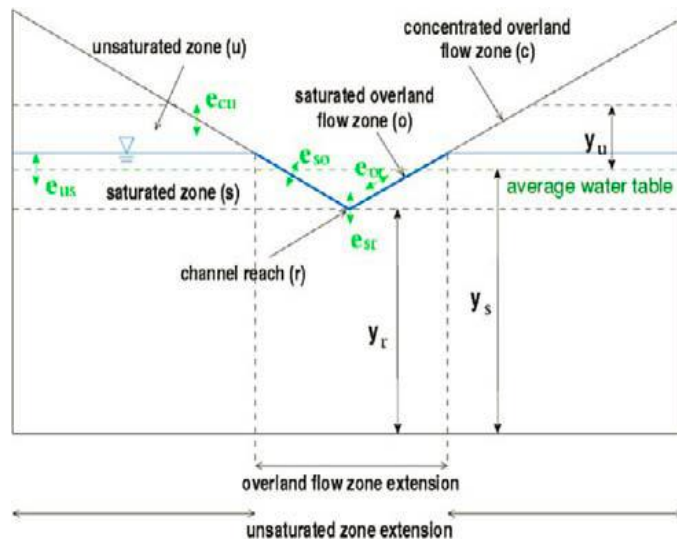


Figure 16: REW cross-section and mass exchange terms (source: (Fenicia et al., 2005))

To enable hydrological variability within a REW, the unsaturated zone can be subdivided into smaller units, and named Representative Elementary Columns (RECs). These RECs can be developed in a GIS interface. Land cover and soil can be taken as an example to create RECs (Reggiani, 2012). On this study RECs are not used.

4.8. Balance equations at the REW-scale

In the REW approach mass, momentum and energy balance equation changed from point to REW scale and explained in the work of (Reggiani & Rientjes, 2005). The resulting conservation equations for mass, momentum and energy have the following general form for each phase and flow zone of a REW (Reggiani & Rientjes, 2005).

$$\frac{d\psi}{dt} = \sum_i e_i^\psi + R + G$$

Where ψ represents a generic property such as mass, momentum or energy, e_i^ψ is a generic watershed-scale exchange term for ψ , R is an external supply term for ψ and G is its internal production. For instance, the mass balance equations that are used for REW model are shown in Table 2. The mass balance equations for unsaturated zone (u-zone), saturated zone (s-zone), the saturated overland flow zone (o-zone), and the channel reach (r-zone) are summarized in the table.

Table 2: Summary of Mass balance equations in REW model (Reggiani & Rientjes, 2005)

Zone	Mass Balance Equations
Unsaturated zone	$\sum \varepsilon \frac{d}{dt}(s^u + y^u + \omega^u) = e^{us} + e^{u top} + e_{wg}^u$
Saturated zone	$\sum \varepsilon \frac{d}{dt}(y^s \omega^s) = \sum_{i=1,N} e^{sm i} + e^{su} + e^{so} + e^{sr}$
Channel reach	$l^r \frac{d}{dt}(m^r) = e^{ro} + e^{rs} + e^{r in} + e^{r out}$
Overland flow	$\sum \frac{d}{dt}(y^o \omega^o) = e^{os} + e^{or} + e^{o top}$

Where: ε , porosity; s^u , REW-averaged saturation of the unsaturated zone; y^u , average depth of the unsaturated zone; ω^u , unsaturated REW area fraction; e^{us} , exchange with saturated zone; $e^{u top}$ Infiltration; e_{wg}^u , Evaporation.

ω^s , dynamics of the saturation overland flow source areas; y^s , REW-averaged saturated zone depth; $e^{sm i}$ Lateral flux through mantle segment i; e^{su} , exchange with unsaturated zone e^{so} , Exfiltration on seepage face; e^{sr} , saturated zone-river exchange

l^r , channel length, m^r , reach-averaged cross section; e^{ro} , Lateral inflow to channel; e^{rs} , Channel-saturated zone exchange; $e^{r in}$, Inflow channel; $e^{r out}$, Channel outflow.

y^o , overland flow depth; ω^o , saturated area fraction ; e^{os} Exfiltration on seepage face, e^{or} , Lateral inflow to channel, e^{otop} , Evaporation from overland flow.

4.9. Parameters and variables

Default parameter sets and some others like water table depth, soil moisture content, channel flow, saturated hydraulic conductivity, soil porosity and the soil retention curve were used for model initialization and understanding the behavior. This was done through running the preprocessor command (Zhang, 2007). The full set of parameterization for REW model is found in the work of Reggiani & Rientjes (2005).

Initial Parameters used for the preprocessor

Steady state base flow event (mm/h):	0.01
Basic hydraulic information	
Overland flow Manning roughness parameter:	0.300
Channel flow Manning roughness parameter:	0.035
Min reach roughness height (mm):	200.0
Max reach roughness height (mm):	200.0
At a station hydraulic geometry	
At-a-station depth scaling exponent:	0.40
At-a-station width scaling exponent:	0.26
At-a-station velocity scaling exponent:	0.34
Down-stream depth scaling exponent:	0.4
Down-stream width scaling exponent:	0.5
Down-stream velocity scaling exponent:	0.1
Down-stream depth scaling coefficient:	0.23
Down-stream width scaling coefficient:	7.09
Down-stream velocity scaling coefficient:	0.61
Discharge-area scaling coefficient:	2e-6
Discharge-area scaling exponent:	0.8
Hydraulic conductivity for channel bed (m/s):	0.00000000001
River bed transition zone thickness (m):	1.5
Saturated overland flow	
Exponent in power relationship (p=1 linear):	0.55
Subsurface	
Water table depth (m):	15.0
Bedrock depth (m):	300
Soil porosity (-):	0.5
Saturated hydraulic conductivity S_{zone} (m/s):	0.0005

Saturated hydraulic conductivity Uzone (m/s):	0.0005
Brooks-Corey soil parameter lambda (-):	0.8
Brooks-Corey pressure scaling parameter (m):	0.25
Initial water content (-):	0.3
Water content at saturation (-):	0.5
Saturated hydraulic conductivity Pzone (m/s):	0.0005
Exponent on transmissivity law ($2 \leq g \leq 4$):	2.5
Depth of saturated subsurface flow layer (m):	0.5
Exponent for surface precipitation partitioning:	0.15
Depth of top soil layer for saturation averaging (m):	0.25

4.10. Evaluation of model performance

For evaluating the performance of the model for simulation, calibration and validation three different objective functions are used in this study: Nash-Sutcliffe Efficiency (NSE), Relative volumetric error and Y (combination of NSE and RVE) will be used. The NSE is a normalized measure (with in a range of $-\infty$ to 1) that compares the mean square error generated by a particular model simulation to the variance of the target output sequence (Schaepli & Gupta, 2007). The NSE is formulated as follows:

$$NSE = 1 - \frac{\sum_{i=1}^n (Qobs_i - Qsim_i)^2}{\sum_{i=1}^n (Qobs_i - \overline{Qobs})^2}$$

Where NSE is Nash-Sutcliffe efficiency, $Qobs$ is the observed discharge, $Qsim$ is the simulated discharge, \overline{Qobs} is the mean observed discharge, and n is the total number of observations.

The RVE is used for quantifying the volume errors and values can vary between $-\infty$ and ∞ . Values within a range of (-5% to +5%) are acceptable in most of the hydrological studies (Janssen & Heuberger, 1995).

The RVE is formulated as follows:

$$RVE = \left(\frac{\sum_{i=1}^n Qsim_i - \sum_{i=1}^n Qobs_i}{\sum_{i=1}^n Qobs_i} \right) * 100$$

Where RVE is a relative volumetric error, $Qobs$ is the observed discharge, $Qsim$ is the simulated discharge, and n is the total number of observations.

Y which the combination function of NSE and RVE which is a measure of overall assessment of the shape of hydrograph and volume is calculated by the equation below (Akhtar et al., 2009). The performance of model simulations for Satellite rainfall estimates forcing was also evaluated with the same objective functions. Y value close to 1 can indicate an excellent performance of the model while lower than 0.6 values indicate poor to satisfactory performance (Rientjes et al., 2013).

$$Y = \frac{NSE}{1 + |RVE|}$$

5. RESULT AND DISCUSSION

In this chapter the findings of this study are presented for each of the objectives proposed in the Introduction section (1). The results are discussed with reference to other scientific works and also compared with findings from previous efforts in the study area and theme.

5.1. Performance of satellite rainfall estimates (SREs) in Upper Gilgel Abay Catchment

5.1.1. Performance of CMORPH

The rainfall estimates acquired from CMORPH product were evaluated based on information from ground measuring stations. Comparison aimed at daily estimates for which descriptive statistics are calculated like mean, standard deviation and coefficient of variation. The period for analysis is from 2006-2010 (1826 days) but only those days with rain estimates larger than 0 for either CMORPH or the rain gauge are selected. Results of the analysis are shown in Table 3.

Based on mean values, Enjibara station indicated a wider difference between gauge and CMORPH when compared to other stations which is 2.39 mm/day. CMORPH underestimates in Adet (1.67 mm/day), Dangila (0.37 mm/day), Sekela (2.01 mm/day), Wetet Abay (1.62 mm/day) and Kidamaja (1.53 mm/day). Mean values for all stations are higher than from CMORPH and thus indicate that, on multi-annual time scale, CMORPH underestimates rainfall systematically across the Upper Gilgel Abay catchment.

Based on standard deviation values, Enjibara, Wetet Abay and Kidamaja stations indicated higher values (> 2 mm/day) while Adet, Dangila and Sekela stations show a standard deviation value of less than 1.79 mm/day. According to statistics of Standard deviation, which is a measure of the spread of the rainfall estimates from the mean, CMORPH underestimated rainfall than the gauge and follows the pattern of mean.

Table 3: Summary statistics of gauge and CMORPH daily rainfall (2006-2010)

stations	Rain estimates	Mean (mm hr.)	Std. dev.	CV	sample size(days)
Adet	CMORPH	5.24	7.27	1.39	914
	Gauge	6.91	9.06	1.31	
Dangila	CMORPH	8.70	10.80	1.24	945
	Gauge	9.07	11.70	1.29	
Sekela	CMORPH	5.77	8.46	1.47	1312
	Gauge	7.78	9.56	1.23	
Enjibara	CMORPH	8.39	10.19	1.21	1105
	Gauge	10.79	12.59	1.17	
Wetet Abay	CMORPH	7.45	10.02	1.35	1031
	Gauge	9.07	12.19	1.34	
Kidamaja	CMORPH	9.66	11.34	1.17	1076
	Gauge	11.20	13.33	1.19	

Coefficient of variation can show the degree of variation from CMORPH and gauge data and is the ratio of standard deviation to mean. As shown in Table 3, less variation is indicated in Kidamaja and Wetet Abay stations than other stations. Less variability is also reported in CMORPH than gauge rainfall estimates, which indicated the less temporal variability of CHORPH that gauge estimates. Overall, since underestimation shows consistency, the systematic error, or bias, can be calculated. Before the CMORPH estimates can be used for rainfall-runoff modeling in this study, bias correction must be applied.

Scatter plot were prepared to get the general impression of how CMORPH rainfall estimates compared with gauge measurements (see Figure 17). A cluster of points which fall in x-axis shows missed hits where satellite misses and gauge indicates rainfall. There are even higher values (>30mm/day) of SREs which are missed by the satellite which indicates the CMORPH will not give a better estimate in high rainfall events. Points which fall in y-axis indicates false hits where no rainfall indicated in the gauge and satellite specifies the value. The false hit does not match with missed biases in pattern and density. The pattern which is observed from the scatterplot also varies spatially. It shows the spatial variations in the performance of CMORPH estimates in Upper Gilgel Abay catchment. In stations Enjibara, Sekela and Kidamaja satellite misses the rainfall which is indicated in the gauge than other station visually. These can be associated with the topography. Sekela and Enjibara stations are located in mountainous areas where elevation is above 2500 m. This clearly shows the poor performance of CMORPH in detecting rainfall in mountainous areas of Upper Gilgel Abay catchment.

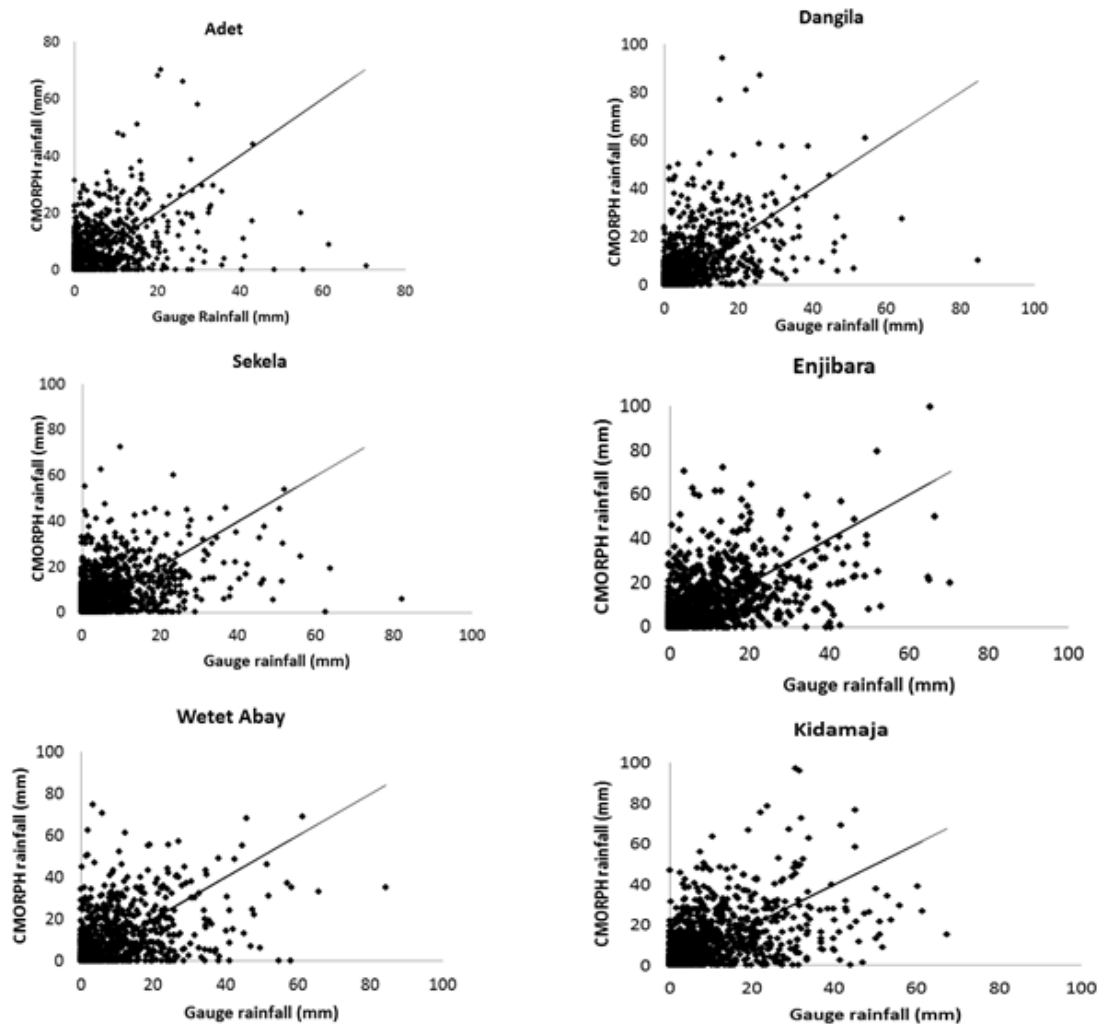


Figure 17: Scatter plots of CMORPH and gauge daily rainfall (2006-2010)

On mean annual time scale, CMORPH underestimates rainfall in all of the stations as indicated in Table 3, which directs the need to apply bias correction before using the CMORPH for modelling runoff. Bias correction selected for this study aimed at correcting both in space and time domains. As indicated in section 4.2 bias factors are estimated for time windows of seven-day time window for each grid element of the CMORPH image so to correct the satellite estimates over space as well. The calculated Bias factors are described in box plot in figure 18 to show the variability and extent of correction factors applied. The ends of Boxes indicate upper and lower quartiles and the horizontal line inside shows the median, while the whiskers show the upper and lower extreme values within 1.5 times the interquartile range (width of the box) from the ends of the box, the red symbols shows outliers.

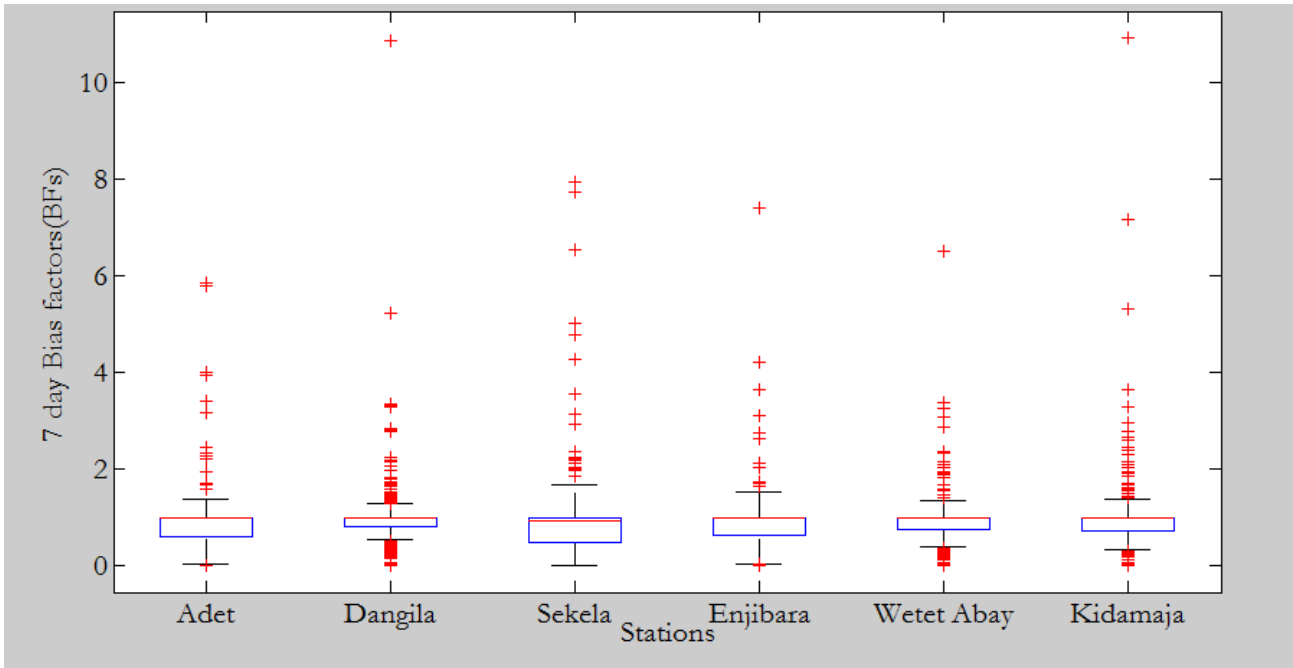


Figure 18: Whisker plot showing comparison of BF'S obtained from 7 days sampling window (2006-2010)

It is found that the lower whisker is at the same level ($BF = 0$) for stations Adet, Sekela and Enjibara, with no outliers found in the lower quartile for Sekela. A wide range of bias factors values are observed for stations Sekela and Enjibara (see figure 18). In Dangila and Kidamaja high BF values (explained in outliers) are reported. The whiskers indicate the extent of bias factors applied in 7-day sampling window. Where a narrow BF's values are applied in Dangila, Wetet Abay and Kidamaja stations. Larger outliers are identified in Dangila and Kidamaja stations. Outliers will contribute in creating the maximum rainfall estimates while using these BF's in bias correction scheme and indicated in Table 4.

5.1.2. Effects of Bias correction

After applying bias correction, findings revealed the bias corrected CMORPH estimates at multi-annual base are closer to the gauge measurements as shown in table 4. For instance, the mean rainfall estimate for Adet in uncorrected CMORPH was 2.62 mm/day and after correction the value changed to 3.04 mm/day which is closer to gauge rainfall (3.46 mm/day). For Enjibara station where there was 1.45 mm/day bias the correction applied reduces the bias to 1.1mm/day. Based on mean statistics the correction applied enhanced the CMORPH estimates in Adet, Enjibara, Sekela and Wetet abay stations (see table 4). The correction scheme which was applied also deteriorated the rainfall estimates in Dangila and Kidamaja stations.

Table 4: Summary statistics of CMORPH daily rainfall before and after TSV bias correction

Stations	Rainfall estimates	Mean (mm/day)	Standard Deviation	Coefficient of Variation	Maximum (mm/day)	Sum	sample size(days)
Adet	Gauge	3.46	7.28	2.103	70.20	6320	1826
	Uncorrected CMORPH	2.62	5.77	2.201	61.65	4786	
	Corrected CMORPH	3.04	6.69	2.199	70.58	5553	
Dangila	Gauge	4.69	9.56	2.037	94.00	8571	1826
	Uncorrected CMORPH	4.51	8.90	1.976	68.15	8226	
	Corrected CMORPH	3.88	7.73	1.993	84.71	7080	
Sekela	Gauge	5.59	8.83	1.579	72.30	10212	1826
	Uncorrected CMORPH	4.15	7.63	1.840	65.35	7570	
	Corrected CMORPH	4.49	8.35	1.862	82.32	8192	
Enjibara	Gauge	6.53	11.12	1.704	99.40	11919	1826
	Uncorrected CMORPH	5.08	8.93	1.758	69.95	9273	
	Corrected CMORPH	5.59	9.77	1.746	70.55	10216	
Wetet Abay	Gauge	5.12	10.21	1.992	74.50	9355	1826
	Uncorrected CMORPH	4.21	8.39	1.994	63.50	7679	
	Corrected CMORPH	4.47	8.88	1.989	84.28	8155	
Kidamaja	Gauge	6.60	11.62	1.761	97.20	12056	1826
	Uncorrected CMORPH	5.69	9.92	1.741	85.35	10399	
	Corrected CMORPH	5.57	9.70	1.741	67.36	10178	

The standard deviation follows the pattern of the mean in all stations. As shown in Table 4, CV values improved in Adet, Dangila and Enjibara stations while in Sekela the value deteriorated when compared to gauge. However, the CV statistics not clearly depicted the improvements like mean and standard deviation when corrected and uncorrected CMORPH are compared. Overall, the underestimation which is reported in section 5.1.1 is improved and mean values are closer to gauge measurements after the correction applied. The pitfall of the correction scheme applied is indicated by the maximum value of rainfall estimate. In Sekela and Wetet Abay the maximum rainfall estimate is increased after applying bias correction (see Table 4).

5.2. REW modelling

5.2.1. Calibration and Validation

Daily streamflow observations for the period 2006-2008 were used to calibrate the REW model. For calibration, the Trial and Error procedure was applied where model parameters are manually changed and optimized with the objective to best simulate the streamflow observation time series. Optimization was done through changing one parameter at a time for each model run to control the effect on model behavior and performance. For calibration only model sensitive parameters are selected as shown in Reggiani and Rientjes (2005). Simple sensitivity was performed for these parameters prior to the actual calibration run. To warm the model for calibration, the year 2005 was selected. The performance of the model for each model run was evaluated with objective functions of Nash-Sutcliffe-Efficiency, volumetric error and a function Y that combines RVE and NSE.

The calibration was done in three steps: first model was run with default model parameters for one year (2005) with *in-situ* measurements of precipitation, evapotranspiration and other climatological parameters for understanding the behavior of the model. The warming up helps to better simulate initial conditions and the simulation was started in the period of low flow which is the month of January.

The second, the model was calibrated for the period 2006-2008 also using rainfall data from the rain gauges. The model parameter values are selected based on literature reviews and changed during calibration with considering their physical meaning in reality. While calibrating getting better match of the base flow between observed and simulated hydrograph was given primary concern. The next emphasis was better simulating peak flows of the observed hydrograph. After getting the better performing model results the precipitation forcing replaced with CMORPH inputs. The focus here is not on improving model simulation result when using SRE but rather comparing of model performance and simulation results when gauge based rainfall is replaced by SREs. More specifically, how well SRE represented the temporal dynamics of streamflow hydrograph like high flows.

Sensitivity analysis of parameters was done with changing highly sensitive parameters (porosity, conductivities) which were identified in many model runs. Thus, the effect of these sensitive parameters in the performance of the model was also assessed. One year (2009) was used for validation of the model with in situ forcing.

5.2.1.1. Model calibration

With the use of the default model parameter sets at the first run, a NS value of 0.12, a RVE of 8.95% and a Y of 0.11 was obtained. The model overestimated discharge with default model run. The simulated base flow not well matched with observed and the Peak discharges are overestimated. The system quickly reacts to rainfall forcing and there is mismatch between simulated and observed discharges especially in wet season. After a number of model runs for calibration, changes in the shape of hydrograph and improvements in Objective functions are noticed while changing some of the parameters. With an increase of exponent of precipitation partitioning from 0.28 to 0.45 and decrease of depth of saturated subsurface flow layer from 0.25m to 0.017 meter a major increase achieved which is NS 0.33 and RVE elevated from 8.95% to -1.70%. These parameter changes dampened of the peak discharges. Further improvement of NS and RVE was achieved with an increase of soil porosity from 0.5 to 0.6 and slight increase of saturated hydraulic conductivity from 0.0005 m/s to 0.008 m/s. With these changes the base flow well matched and the time to peak of some portions of the hydrograph in the beginning of dry season better matched.

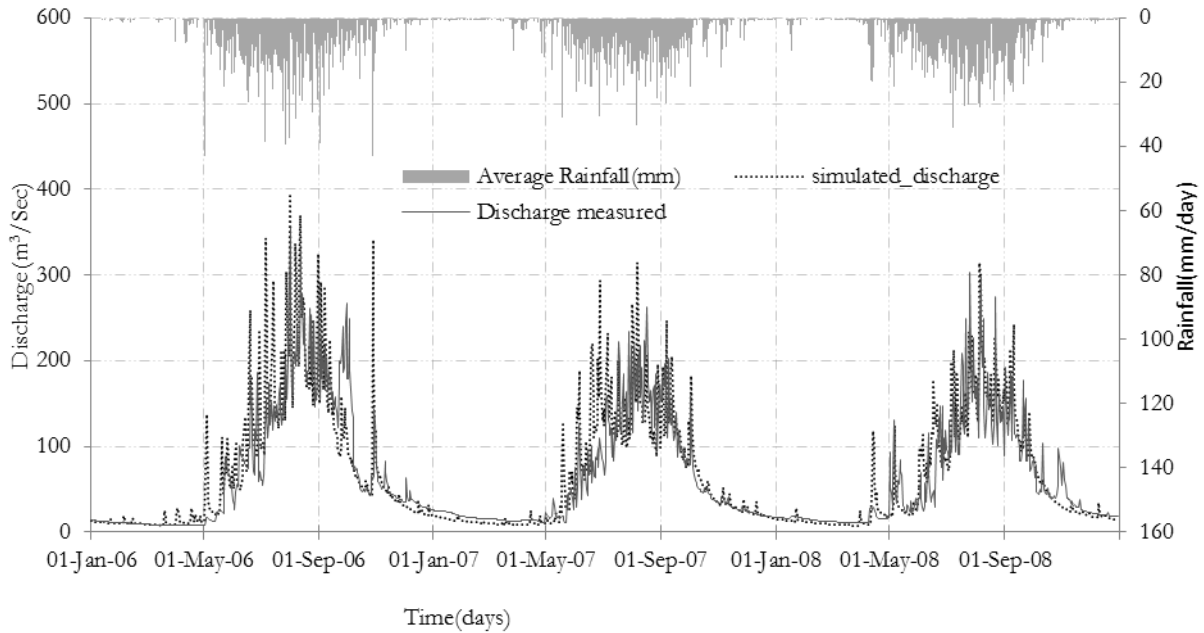


Figure 19: Hydrograph showing the calibration result for 2006-2008

Results of model calibration are shown in Figure 19. Objective function values for final calibration are 0.71 for NS, 4.07% for RVE and 0.68 for Y. Values as such indicate a satisfactory model performance. Characteristic to the hydrographs are the relatively high discharges after periods of high intensity rainfall. The total Mass Error reported in the model simulation turns in to 2.4×10^{-9} after three year model run and indicates that all mass tracked and traced during a simulation. As shown in figure 19, the model simulates the initial condition and base flow well. The rising limb and recession limb are reasonably similar to the observed discharge. Most of the peak discharges in the year 2007 and 2008 are also simulated well. The model simulates peak flows in months of May and November (see figure 19) which can be associated with high precipitation events indicated but not shown in observed hydrograph. In contrast, it simulates some peaks which are not shown in the observed hydrograph. These might be associated with missing the high flows within these days in measuring or model structure. Overall, it can be concluded as base flow is well simulated for entire hydrograph. The peak discharges are also simulated well except some mismatches observed.

5.2.1.2. Sensitivity Analysis

For sensitivity analysis many model runs were conducted to identify the parameters which are highly sensitive together with the referring the results of earlier works (e.g. Reggiani & Rientjes, 2005 and Zhang, et al., 2006). Three year model run which is similar to calibration was used for the sensitivity analysis. Highly sensitive parameters were changed manually at a time keeping less sensitive parameters unchanged. Finally, six cases which are close to the calibrated parameter sets in the performance selected and shown in Table 5. The result revealed that the model is highly sensitive to saturated hydraulic conductivities and porosity (soil parameter). It is also sensitive to depth of saturated subsurface flow layer. It is found that keeping the soil porosity similar and slightly increasing Ksat (see Table 5: cases I, II and II), enhances the model performance which allows better reproducing the peak flows of the hydrograph. In cases III and VI, the soil porosity increased from 0.45 to 0.6 (which creates more storage to the system) and by keeping Ksat unchanged, the NS improved from 0.69 to 0.71. The sensitivity analysis results revealed subsurface parameters such as porosity and hydraulic conductivities are sensitive in affecting how well the model can simulate the stream flow discharges in Upper Gilgel Abay catchment.

Table 5: Sensitivity analysis (2006-2008)

Model consistency	Soil porosity(-)	Saturated hydraulic conductivity (Ks)(m/s)	NS (Nash-Sutcliffe-Efficiency)	RVE (Relative volumetric error) (%)	Y
Case I	0.45	0.004	0.67	-7.02	0.63
Case II	0.45	0.015	0.67	13.00	0.59
Case III	0.45	0.008	0.69	2.64	0.68
Case IV	0.6	0.001	0.59	-17.44	0.51
Case V	0.6	0.004	0.69	-5.52	0.65
Case VI	0.6	0.008	0.71	4.07	0.68

5.2.1.3. Model Validation

Because of the inter-annual rainfall variation and missing values observed in the year 2010 and 2011 only one year (2009) was used for validation of the model with rainfall inputs from rain gauges. For validation, the optimized parameter set by the calibration is used. Validation results indicate satisfactory model performance with objective function values for NS 0.62 and for RVE 9.59%. The latter indicates a relative high, positive, volumetric error. For the combination function Y a value of 0.57 was obtained, may be considered satisfactory. As shown in figure 20, the simulation result, peak flows and low flows are not always accurately simulated. However, the simulated hydrograph follows the general shape of the observed hydrograph.

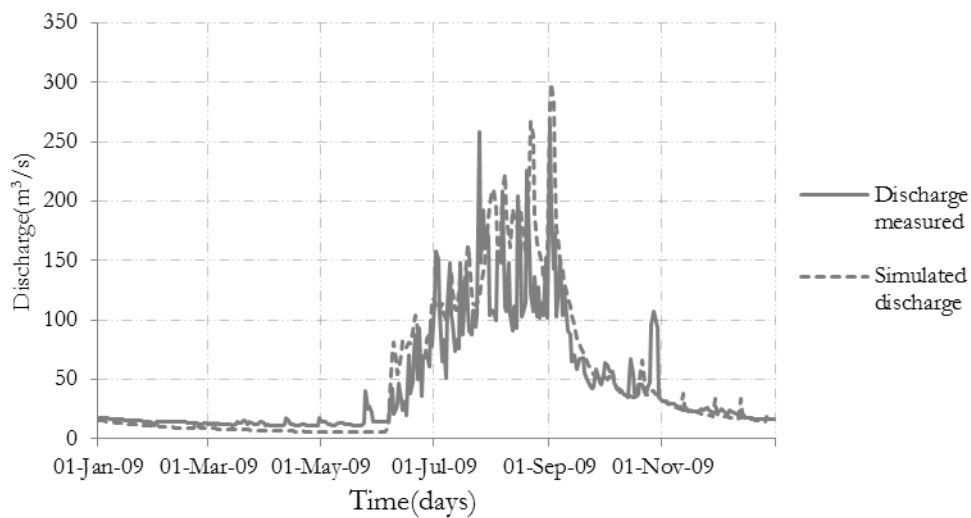


Figure 20: validation hydrograph for the year 2009

5.3. Runoff simulation with satellite rainfall estimates forcing

CMORPH rainfall estimates were used as input to the REW as forcing term to evaluate how well the observed hydrograph can be simulated. Similar to the use of rainfall time series from rain gauges for model calibration, for the same period bias corrected CMORPH estimates are used. Results of modelling were evaluated by means of NS, RVE and Y is shown in Table 6.

Table 6: Performance of CMORPH on runoff simulation

forcing	NS(Nash-Sutcliffe-Efficiency)	RVE (Relative volumetric error) (%)	Y
CMORPH(2006-2008)	0.57	0.80	0.56
CMORPH(2006-2010)	0.43	13.71	0.38
CMORPH 2008	0.52	-4.81	0.50
CMORPH 2010	0.36	15.30	0.31

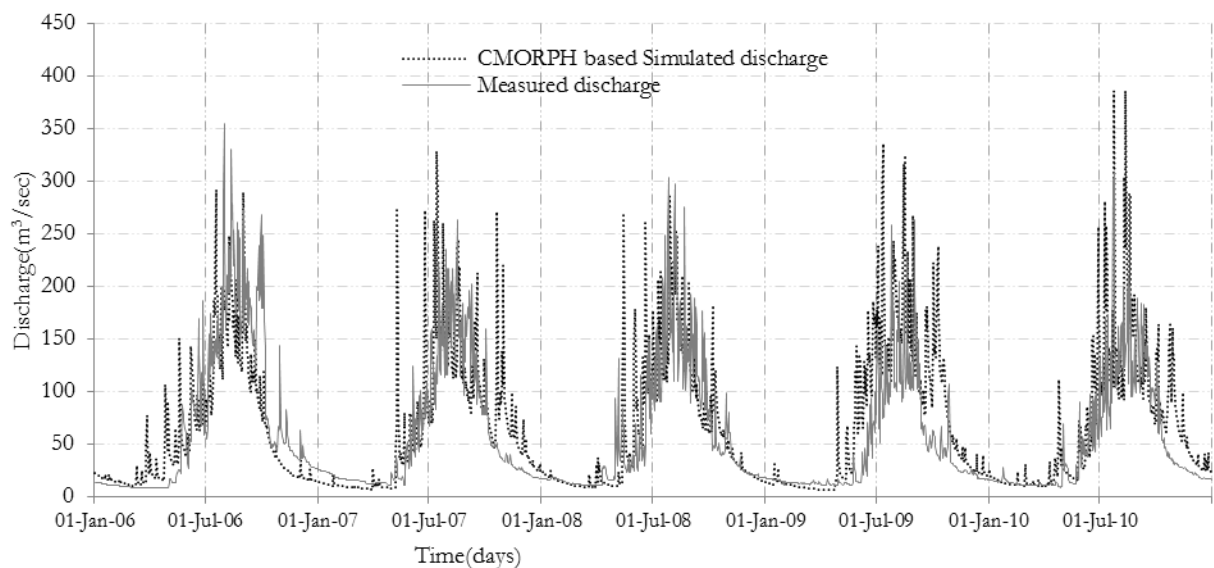


Figure 21: Streamflow simulation with bias corrected CMORPH rainfall estimates (2006-2010)

Based on the simulation result found, the base flow and most of the peaks follow a pattern of the observed hydrograph. Peaks for the years 2007-2010 are relatively well simulated (see figure 21). For the year 2006, the simulated hydrograph does not match with the measured discharge in many aspects like peak flows, rising limb and recession limb. For years 2007, 2009 and 2010, model simulation results do not well match for the rising and recession limbs as shown in measured streamflow (see figure 21). Recession starts much quicker for measured data for 2007, 2009 and 2010 indicating that SRE rainfall extends for a longer period compared to gauged rainfall. These differences in the model performance annually can be associated with the inter-annual rainfall variations and the difference in the performance of the satellite in detecting rainfall. A better performing model in simulating runoff is shown when using shorter time series (3) years (see Table 6).

To better evaluate inter-annual differences in SREs year 2008 (that seems visually better) and 2010 (that appears to be poorer), are plotted in figure 22, left and right respectively. The year 2008 shows better results of NS (0.52) and RVE (-4.81). In 2008 higher peaks are shown at the start of the wet season but with good recession part. In 2010 rising limbs are better represented and the highest peaks are shown with mismatches (See also to Fig 22 for these patterns). The overall shape of the hydrograph also preserved well for the year 2008, where NS (0.52) and RVE (-4.81%) was obtained. While evaluating the year 2010 only, NS (0.36) and RVE (15.3%) was found, which can be taken as poor performance when compared to 2008. Overall, the performance of SREs follows the shape of stream flow hydrograph measured but varies annually.

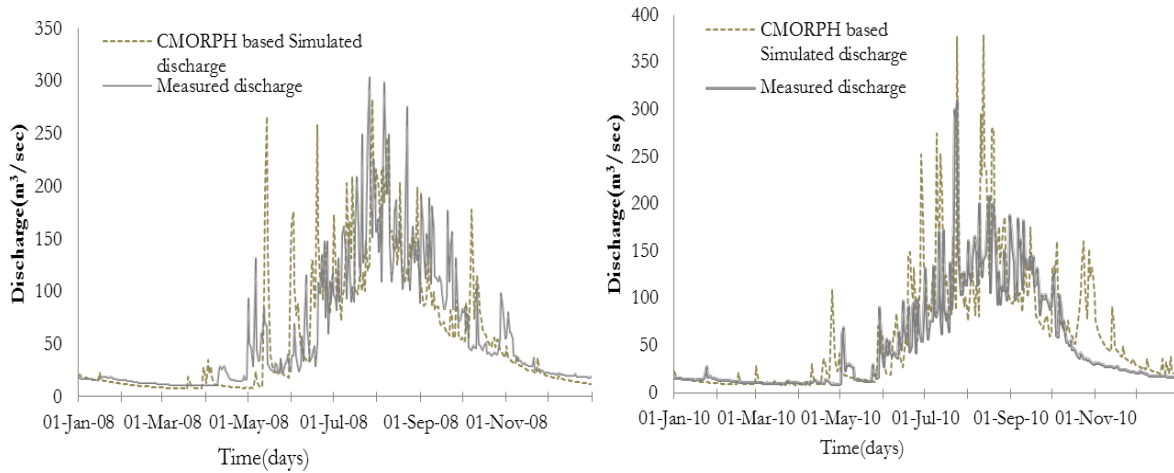


Figure 22: Stream flow simulation with bias corrected CMORPH rainfall estimate (left; for the year 2008; and right; 2010)

5.4. Identification of major runoff source with in the catchment

Saturated excess overland flow is the contribution of runoff which is generated from the saturated component of the REW areas. Rainy months of June, July, August and September (end of wet season) was taken for identifying the daily saturated excess overland flow contribution to the streamflow. The *in-situ* based streamflow simulation result was selected from SREs for analysis because of better model performance.

Results of analysis of saturation excess overland flow are show in Figure 23 where for each REW (1-33) the overland flow depths is shown for the period 12 months (June, July, August and September 2006-2008). Average Depths result from accumulating the daily simulated overland flow depth was considered for analysis to indicate the REWs that mostly contribute to streamflow by saturation excess overland. The average depth ranges from 0-0.106 mm/day and REWs close to the river reaches are identified as high saturation excess generating areas (see figure 24).

Areas in southern (REWs 19,20,21,22and 23) and south western(REWs 7,11,12 and 15) part of Upper Gilgel Abay catchment indicated an average saturated overland flow thickness of 0.018-0.051mm and in mountainous areas of REW 16,29 and 30 a value lower reported(0-0.018 mm). Hence, spatial differences in signals of saturated excess overland flow identified with REW approach in Upper Gilgel Abay catchment.

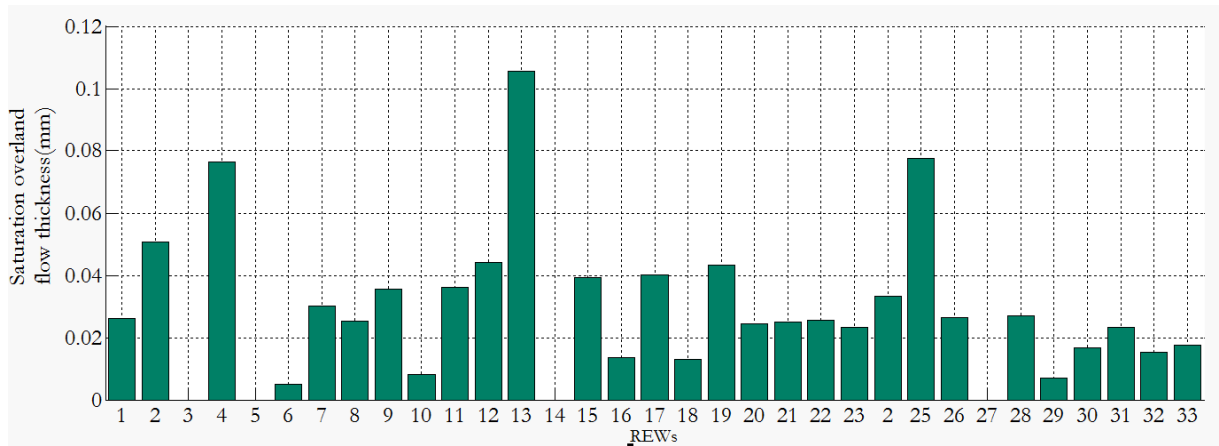


Figure 23: Average Saturation excess thickness (mm) for REWs for wet season (months of June, July, August and September 2006-2008) per day

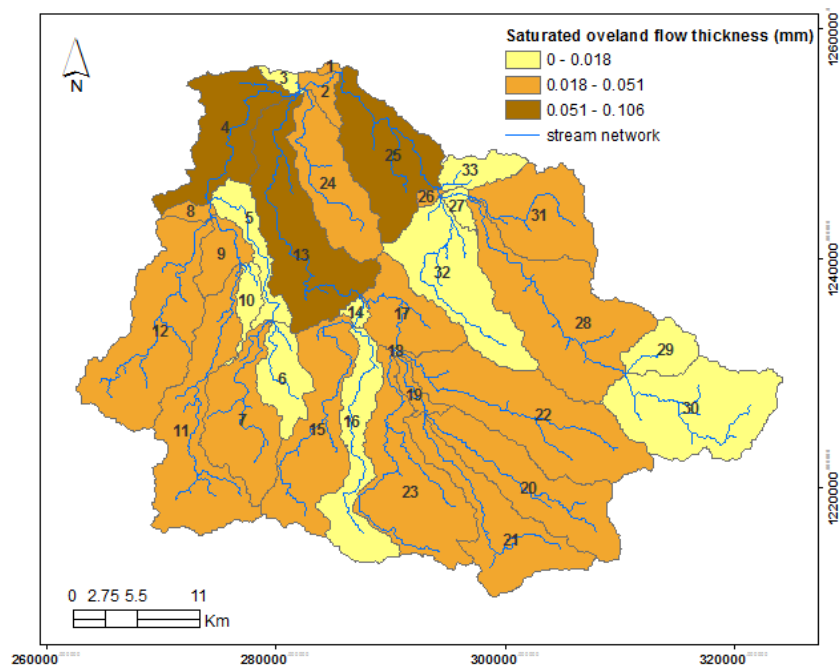


Figure 24: major runoff generation (saturation excess) source REWs

Three REWs (4, 13 and 25) selected for analysis, which generate high saturation excess overland flow compared to other REWs and displayed in Figure 24. REW 4 has area of 64.46 km² which is 4.1 % of the total area of the catchment and is located in lowest elevation ranges 1918-2160m. REW 13 have area of 101.10 km² which is larger area than the other two selected REWs (covers 7% area and found in elevation ranges of 1918-2214m). REW 25 also follows the other two. REW 25 has area of 75.21 km² (covers 4.78 % and characterized as low elevation area (1896-2181m) compared to other REWs)). What makes all 3 REWs is the fact that these areas are very close to the outlet and river reach. For further analysis of where these REWs are located see Figure 24.

Can locations of saturated excess overland flow areas be related to rainfall distribution?

Average daily rainfall for the rainy months of June, July, August and September 2010 are plotted combined with average saturated excess overland flow from REWs 4, 13 and 25 that show highest saturation excess runoff (figure 25). A well-defined relation between rainfall and runoff is not shown although some days with high intensity rainfall also show high saturation excess runoff. However the result on the relation is somehow expected since the main driver for saturated excess overland flow is not rainfall rather it is associated with water table increase and when the water level reaches land surface and appears in the form of exfiltration. The correlation between average rainfall and saturated excess overland flow shows 0.0009, which indicates very little to no association (see figure 26).

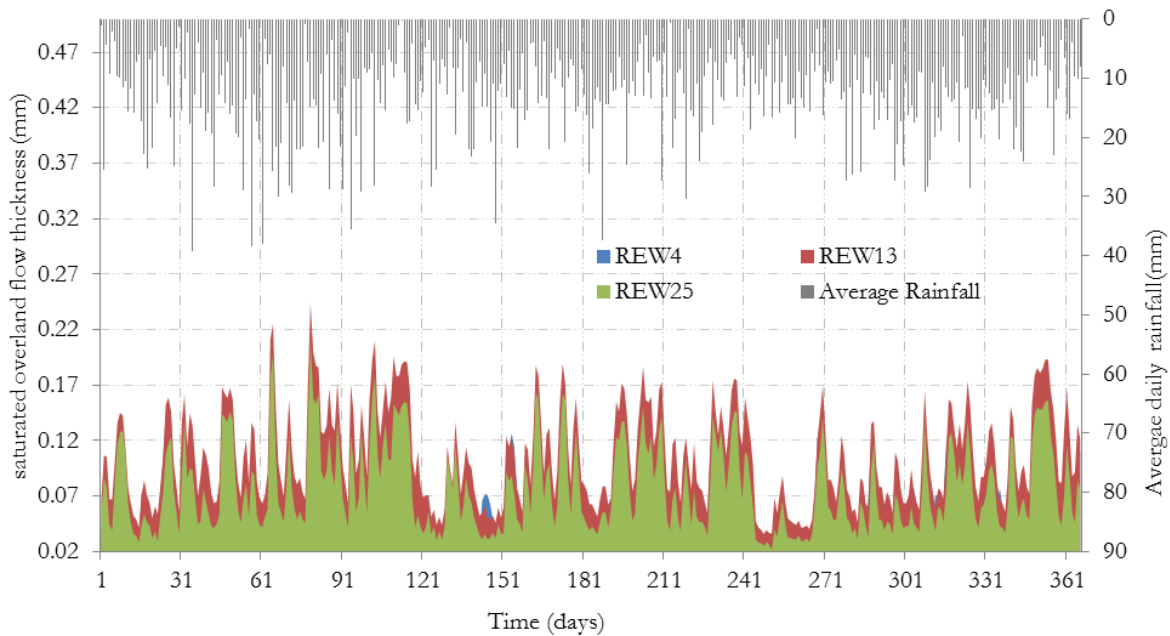


Figure 25: Simulated saturated excess overland flow thickness for REW 4, REW 13, and REW 25

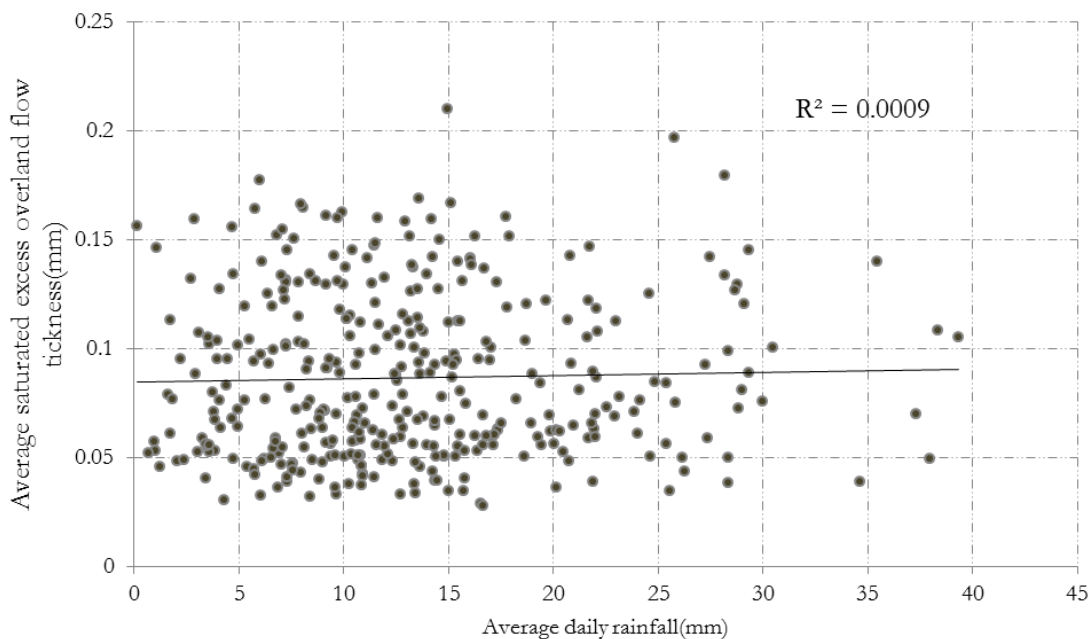


Figure 26: Correlation of REW average daily rainfall and Simulated saturated excess overland flow for REW 4, REW 13, and REW 25

5.5. Comparison of high temporal resolution (hourly) and daily forcing on runoff simulation

Temporal variability of rainfall with in Upper Gilgel Abay catchment reported in previous works as indicated in the background section. In this work CMORPH 8km \times 8km and 1hr product was aggregated in to daily and used as forcing for stream flow simulation as discussed in section 5.2.3. However, hourly SRE was not tested as input for modelling stream flow in REW approach. The hourly simulation was done with keeping parameters and other climatological parameters similar to the respective daily time step. The analysis was done for three rainy months (June, July and August) of 2010, to better examine the difference in rainy season where differences in time step can be clearly observable on simulation. The resulting stream flow hydrograph for hourly time step is shown in figure 27. The result clearly shows the impact of time scale in the shape of stream flow hydrograph. The volumetric error found was -3.39%. This value can be taken as acceptable to make the comparison of the shape differences of the hydrograph. Average Lag time of 12.5 hours was found for 5 of the highest peaks observed in hourly simulation. The visual inspection of hourly simulation typically shows high flows which are not depicted in daily simulation and gauge measurements. These peaks are associated with high intensity rainfall event which last for short period and generate peak flows which might be missed during measurement. Aggregation of rainfall hourly SREs also totalizes these events as simple summation was used for daily time step. Overall, the shape of hourly simulation follows daily simulation as depicted in figure 27.

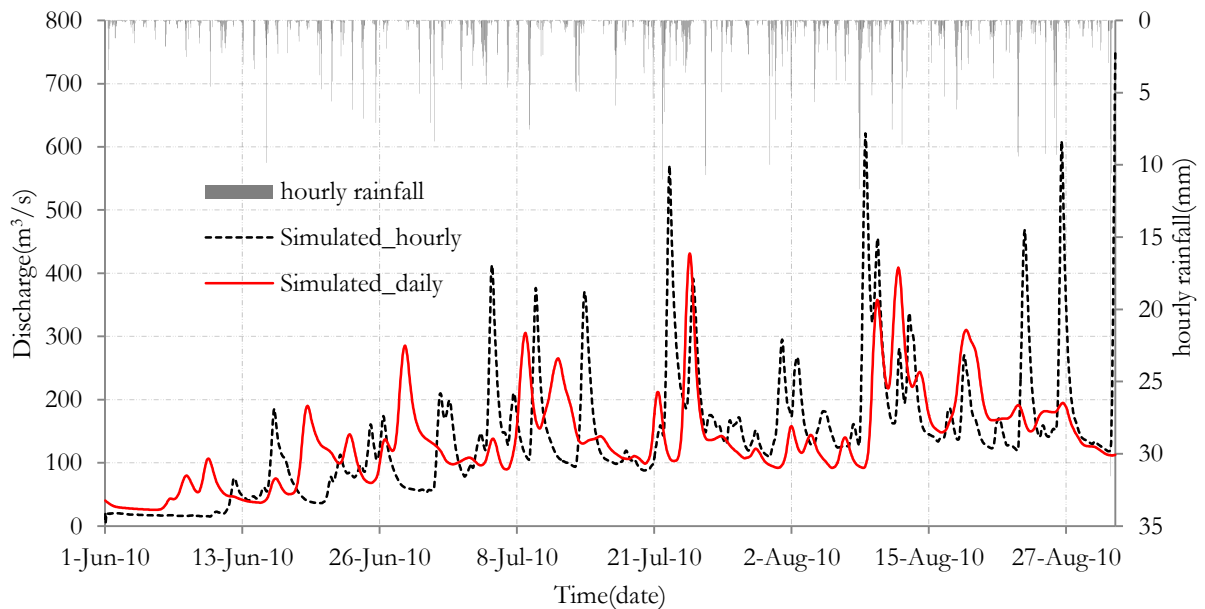


Figure 27: Comparison of hourly and the daily forcing on runoff simulation (June, July and August 2010)

To better investigate the differences between hourly and daily SREs based simulations exceedance probability graphs was plotted and shown in figure 28. Exceedance probability defines the percentage of time that a given discharge can be equaled or exceeded. All simulated values were plotted in figure 28 to better capture the differences. The exceedance plots show clear differences in hourly and daily based simulations in peak flows and low flows (see figure 28). The differences in distribution of simulated values are evident for exceedance probabilities of <20% which is associated with 200 m³/s discharge, which shows a difference in high flow simulation caused by time step differences in forcing. In hourly simulation, there is a probability of getting even higher than 500m³/s discharges which are not indicated in daily time step. The result revealed the probability of occurrence of high flows for daily CMORPH is lower than hourly CMORPH based simulation. For low flows, the difference in distribution starts for discharges less than 100m³/s which are associated with the exceedance probability of 73%. This can be

associated with the finer time step rainfall tested in modeling which can also depict the response in generating very high peaks in the hydrograph.

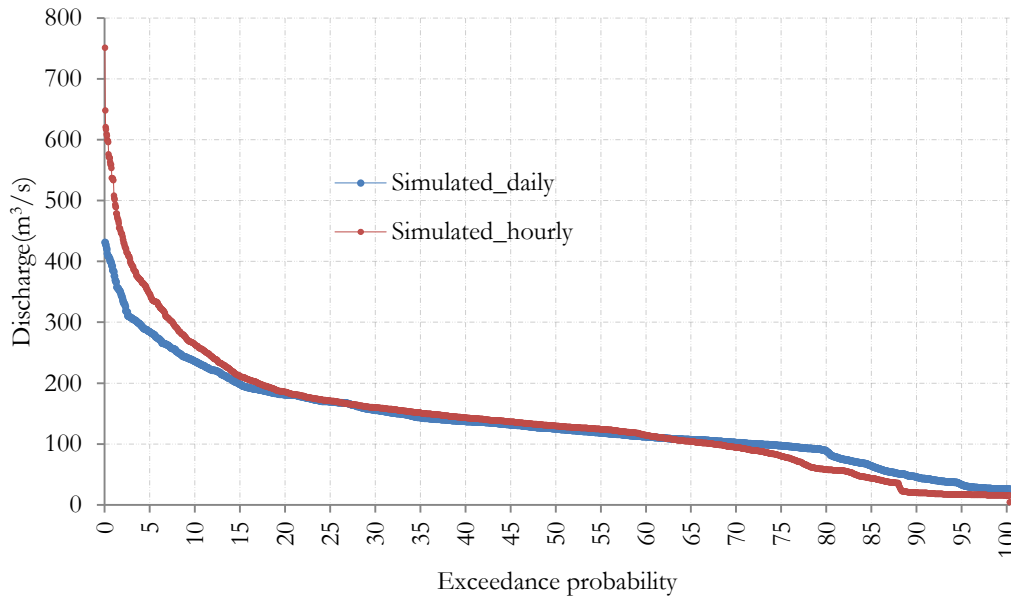


Figure 28: Exceedance probability graph

In Upper Gilgel Abay catchment daily streamflow measurements are taken once at 8:00 AM in the out let. Hence to examine the actual differences between simulated hourly and measured discharge, comparison was done at similar time of the day. The hourly simulation result at 8:00 AM for each day compared with daily streamflow observations which are taken at 8:00 AM hour. The difference was evaluated based on objective functions RVE, NS and Y. Objective function value of -0.82 for NS, 8.29% for RVE and -0.76 for Y were obtained. Values as such indicate a poor model performance. Characteristic to the hydrographs are the relatively high discharges simulated for hourly CMORPH than daily measured at similar time of the day. This can be associated with the finer modeling time step which was applied in hourly based simulation. The rainfall forcing given to the model shows quicker response in the model while using hourly than daily based simulation. Hence, the diurnal variability can be simulated with finer time step SRE data, which is not measured in the field. However, the poor model performance resulted from using hourly CMORPH data and lack of sub daily discharge measurement has constrained the test simulation conducted.

5.6. Discussion

Representative elementary watershed approach is tested in Upper Gilgel Abay catchment to simulate the dynamics of runoff with satellite rainfall estimates forcing. CMORPH (1-hr, temporal and 8 km × 8 km spatial resolution) product was selected based on previous inter-comparison studies in Lake Tana basin. Based on the findings of this study, CMORPH underestimates rainfall up to 18% during the analysis period (2006-2010). Spatially, there are clear variations on the performance of CMORPH across rain gauging stations. For instance, Station Dangila showed a smaller range of biases (see figure 20) and Enjibara which is located at the top of mountain indicated higher bias between gauge and CMORPH when compared to other stations. This indicates the impact of topography on detection and performance of satellite rainfall estimates. Similar findings was reported by Haile et al. (2013).

SREs are not direct measurements of rainfall like gauges and they are contaminated with random and systematic errors which affects their applicability. Hence, time and space variant bias correction algorithm was applied to minimize the systematic errors or bias of CMORPH product. The algorithm was tested effective in similar catchment by the Habib et al. (2014). The correction scheme has improved the SREs in most of the stations, but it has also deteriorated in some stations. Bias corrected CMORPH rainfall estimates were used as forcing to evaluate how well observed hydrograph can be reproduced, and the result obtained can be taken satisfactory with 3 year time series. As shown in figure 29, for 3 year time series data, Insitu and CMORPH based streamflow simulations are plotted to explore the basic similarities and differences that are observed. In both hydrographs as shown in figure 29, the base flow and the pattern of the hydrograph are captured. Based on objective function evaluations Insitu based simulations has indicated better performances (see section 5.2 and 5.3) than CMORPH based streamflow simulations. This difference can be associated with the calibration procedures that were applied. The model was calibrated with insitu data. Hence a better performing model could be obtained if the model is recalibrated with CMORPH data. Bitew et al. (2012) also indicated a best-performing model simulation after bias correction and model recalibration.

Through visual inspection, the main difference is the longer recession (except year 2006, where both failed to simulate well and possibly associated with model structure) and rising limb observed while using CMORPH based than in situ based simulations. It indicates that SRE rainfall for some years extends for a longer period compared to gauged rainfall. Most of the peak flows were better captured with Insitu than CMORPH based streamflow simulations. Peaks are not well simulated with CMORPH input for years 2006 and 2007(see figure 29) but are reasonably in agreement with measured for 2008 with some mismatch. The overall difference observed between Insitu and CMORPH based streamflow simulations can be caused by different factors such as the poor distribution of reference rain measuring stations that were used to correct CMORPH, the point (gauge location) to pixel (grid element) comparison which were applied in calculating the bias factors, the deficiencies of bias correction algorithm and the CMORPH error which is not totally removed after correction applied. The poor performance of CMORPH was also reported in Upper Gilgel Abay catchment with daily forcing (25 degree spatial resolution which is much coarser than the one used in this study), and through MIKE SHE model and found 0.34 NS (Bitew et al., 2011).

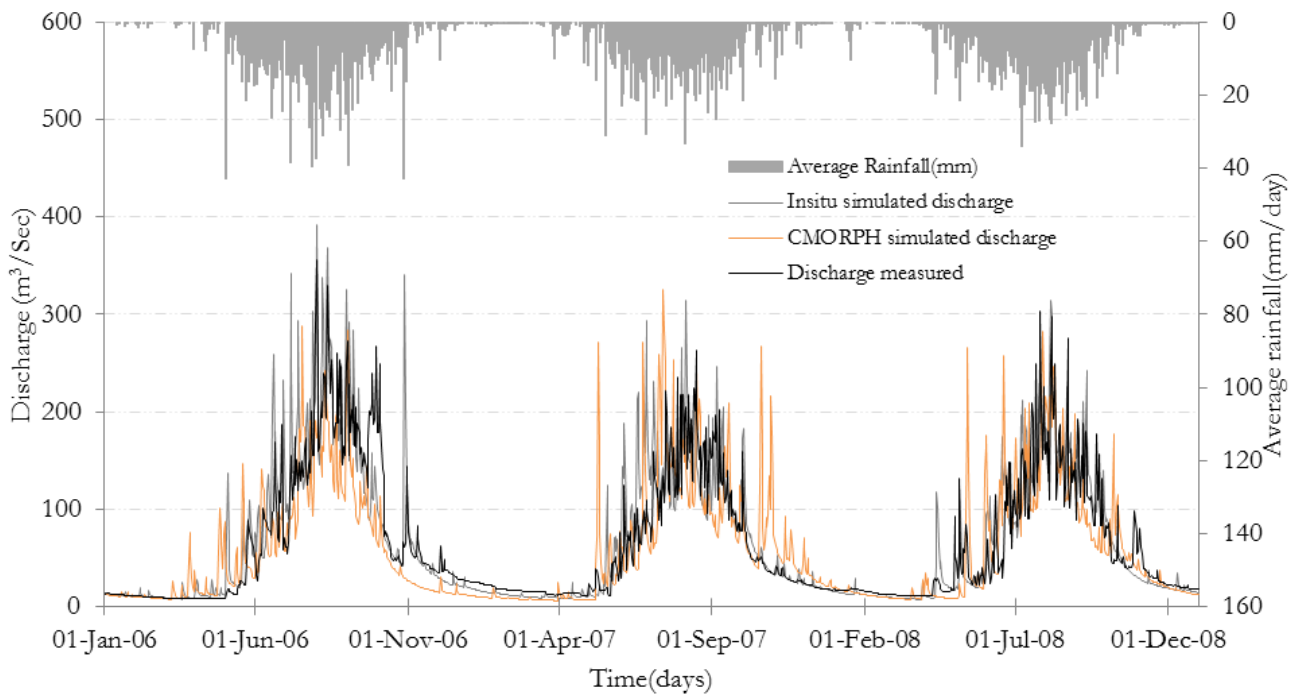


Figure 29: Streamflow simulation with bias corrected CMORPH and Insitu rainfall estimates(2006-2008)

In the same catchment, the performance of CMORPH 25km and 3 hourly product was evaluated in stream flow simulation through SWAT model and found simulations capture remarkably the observed stream flow hydrographs and indicated inter-annual differences where lower performance in 2007 than in 2006 (Bitew & Gebremichael, 2011). The issue of inter-annual differences is important when working with SREs because their ability to distinguish between wet and dry years is inherent in the raw data product. It is difficult to correct for such shortcomings without an extensive overlapping of rain gauge dataset (Stisen & Sandholt, 2010). Inter-annual differences in performance of SRE clearly were also shown in this study as discussed in section 5.2.3.

From simulation results, areas which generate high Saturation excess runoff are found very close to the outlet and river reach. These areas are situated in relatively flat terrain. This result is similar to Zhang et al. (2005) where REWs with higher slope angle produce smaller VSA and these areas are adjacent to the river valley and tend to be flatter thus generating larger VSA than those in the upstream with a steeper slope. On the other hand, no clear pattern found between saturated overland flow and rainfall distribution in Upper Gilgel Abay catchment.

In Upper Gilgel Abay catchment discharge measurements are available on daily time step; hence, 1-hr CMORPH product was aggregated with simple summation for daily CMORPH based streamflow simulations. While aggregating hourly SREs, the diurnal variability of rainfall which possibly has an impact on shape of stream flow hydrograph is ignored. On the contrary, temporal variability of rainfall within a day can have an impact on the runoff behavior. Frequent rainfall and convective activity were observed in the afternoon over the southern mountains and in the night over the southern part of the Lake Tana shore (Haile et al., 2009). To understand runoff behaviour at sub-daily time step in Upper Gilgel Abay catchment efforts were done in this work by comparing daily with hourly stream flow simulation with SRE input. The findings show that hourly based simulated hydrograph creates peak flows which are not depicted in daily simulation. With the use of distributed model and hourly modelling time step changes in shape of the hydrograph such as a shift in time to peak, an increase in height of the some peaks and a

decrease in some lower flows are depicted. This component of the research is constrained by lack of sub-daily discharge measurement for verification of simulation results.

6. CONCLUSION AND RECOMMENDATION

6.1. Conclusions

In this study the performance of 1-hr temporal and 8 km × 8 km spatial resolution CMORPH rainfall product has been evaluated over Upper Abay catchment for reproducing the stream flow measurement at the outlet through REW model. Hydro-meteorological data obtained from seven stations in and outside the catchment area were used as ground references for bias correcting CMORPH data before using for modelling. The modelling work was conducted for 5 years (2006-2010) to better evaluate the performance of SREs over time. Statistical techniques of mean, standard deviation and coefficient of variation were used to evaluate the performance of SREs before and after bias correction. Objective functions like NS, RVE and Y were applied to assess how well the stream flows were reproduced in simulations. The conclusions deduced from findings are the following as of the objectives:

1. CMORPH SREs has underestimated rainfall systematically (up to 18%) throughout the catchment. Spatially, there are clear variations identified on the performance of CMORPH across rain gauging stations, where in Dangila station SREs has performed better and in Enjibara and Sekela stations relatively higher biases are found. This can be associated with the impact of topography on the performance of SREs as Enjibara and Sekela stations are located in the mountains. The applied bias correction scheme (time and space variant) has reduced the systematic errors of CMORPH, and improved the underestimation reported in most of the stations.
2. Lower model performance is reported while using satellite rainfall estimates instead of rainfall data from rain gauges. The performance of SREs based simulations captures the shape of stream flow hydrograph measured. Based on the simulation result, the initial condition, base flow and most of the peaks followed a pattern of the observed hydrograph. The model performance varies annually and seasonally and these differences can be associated with the inter-annual rainfall variations observed and the difference in the performance of the satellite in detecting rainfall. A better performing model in simulating runoff identified while using shorter time series (e.g. 2006-2008) than the actual simulation period (2006-2010).
3. With REW approach, the model simulations have identified signals of saturated excess overland flow depth. Relatively high average signals identified in areas which are close to river reach and the outlet. Three REWs (4, 13 and 25) generate high saturation excess runoff compared to other REWs. Areas in southern and south eastern part of the catchment showed less average saturated excess overland flow than Northern part and these areas are mountainous. The source for saturation excess overland flow is not directly from rainfall distribution rather it is from saturated domain.
4. In examining the diurnal variability of stream flow, hourly CMORPH rainfall estimates based simulation typically detect high flows which are not indicated in daily simulation and gauge measurements. These peaks are associated with high-intensity rainfall event which lasts for a short period and generates peak flows which might be missed during measurement. Hence, the finer time step rainfall (hourly) has generated high peaks while daily simulation suppresses the shape of the hydrograph. Thus, with high temporal resolution satellite rainfall (1-hr) additional information regarding the diurnal variability of stream flow can be obtained.

6.2. Recommendations

- CMORPH SREs at high spatial and temporal (1-hr and 8 km × 8 km) resolution has reasonably represented rainfall amount and distribution after bias correction. Hence combining SREs with gauge measurement may lead to get advantage of information from both gauge and satellite rainfall estimates for using for hydrological modelling.
- In this study, the focus was on comparing gauge and satellite based rainfall forcing in their impact to simulate stream flow hydrograph. As reported in result section satellite rainfall estimate based simulation does not perform well like gauge based simulation. Hence, a best-performing model might be obtained after applying other bias correction algorithms which are not used in this study like correction for topography. Model recalibration with SRE forcing may also improve model performance (NS and RVE values) while using satellite rainfall for streamflow simulations.
- The findings of Hourly CMORPH rainfall based stream flow simulation showed much higher peak flows which are not depicted in daily simulation. This result can be taken as insight to other researches on simulating the diurnal variability of stream flow in Lake Tana basin. This theme is recommended for future works by taking reasonable time series for hourly rainfall based steam flow simulation.

LIST OF REFERENCES

- Abatzoglou, J. T., Redmond, K. T., & Edwards, L. M. (2009). Classification of regional climate variability in the state of California. *Journal of Applied Meteorology and Climatology*, 48(8), 1527–1541. doi:10.1175/2009JAMC2062.1
- Akhtar, M., Ahmad, N., & Booij, M. J. (2009). Use of regional climate model simulations as input for hydrological models for the Hindukush-Karakorum-Himalaya region. *Hydrology and Earth System Sciences*, 13(7), 1075–1089. doi:10.5194/hess-13-1075-2009
- Al, J. E. T., Joyce, R. J., Janowiak, J. E., Arkin, P. a., & Xie, P. (2004). CMORPH: A Method that Produces Global Precipitation Estimates from Passive Microwave and Infrared Data at High Spatial and Temporal Resolution. *Journal of Hydrometeorology*, 5(3), 487–503. doi:10.1175/1525-7541(2004)005<0487:CAMTPG>2.0.CO;2
- Alemohammad, S. H., McColl, K. A., Konings, A. G., Entekhabi, D., & Stoffelen, A. (2015). Characterization of precipitation product errors across the United States using multiplicative triple collocation. *Hydrology and Earth System Sciences*, 19(8), 3489–3503. doi:10.5194/hess-19-3489-2015
- Allen, R. G. (1998). FAO Irrigation and Drainage Paper Crop by. *Irrigation and Drainage*, 300(56), 300. Retrieved from <http://www.kimberly.uidaho.edu/water/fao56/fao56.pdf>
- Anagnostou, E. N., Maggioni, V., Nikolopoulos, E. I., Meskele, T., Hossain, F., & Papadopoulos, A. (2010). Benchmarking high-resolution global satellite rainfall products to radar and rain-gauge rainfall estimates. *IEEE Transactions on Geoscience and Remote Sensing*, 48(4 PART 1), 1667–1683. doi:10.1109/TGRS.2009.2034736
- Beven, K. J. (2012). *Rainfall-runoff modelling*. Wiley-Blackwell (Second Edi.). Lancaster University, UK. doi:10.1002/9781119951001
- Bitew, M. M., & Gebremichael, M. (2011). Assessment of satellite rainfall products for streamflow simulation in medium watersheds of the Ethiopian highlands. *Hydrology and Earth System Sciences*, 15(4), 1147–1155. doi:10.5194/hess-15-1147-2011
- Bitew, M. M., & Gebremichael, M. (2011). Evaluation of satellite rainfall products through hydrologic simulation in a fully distributed hydrologic model. *Water Resources Research*, 47(6), 1–11. doi:10.1029/2010WR009917
- Bitew, M. M., Gebremichael, M., Ghebremichael, L. T., & Bayissa, Y. a. (2012). Evaluation of High-Resolution Satellite Rainfall Products through Streamflow Simulation in a Hydrological Modeling of a Small Mountainous Watershed in Ethiopia. *Journal of Hydrometeorology*, 13(1), 338–350. doi:10.1175/2011JHM1292.1
- Buytaert, W., Celleri, R., Willems, P., Bièvre, B. De, & Wyseure, G. (2006). Spatial and temporal rainfall variability in mountainous areas: A case study from the south Ecuadorian Andes. *Journal of Hydrology*, 329(3-4), 413–421. doi:10.1016/j.jhydrol.2006.02.031
- Cao, W., Bowden, W. B., Davie, T., & Fenemor, A. (2009). Modelling impacts of land cover change on critical water resources in the Motueka River Catchment, New Zealand. *Water Resources Management*, 23(1), 137–151. doi:10.1007/s11269-008-9268-2
- Dagninet Moges, D. (2008). *Land surface representation for regional rainfall-runoff modelling, upper Blue Nile basin, Ethiopia*.
- Davie, T. (2008). *Fundamentals of Hydrology, Second Edition. Management* (Vol. 298). Retrieved from <http://books.google.com/books?hl=en&lr=&id=x0HfA6HJvogC&oi=fnd&pg=PP1&dq=Fundamentals+of+Hydrology&ots=fi3rcmkBRZ&sig=xXLEc2AGr243RS1Iqr6q66rbyFM>
- Dessie, M., Verhoest, N. E. C., Pauwels, V. R. N., Admasu, T., Poesen, J., Adgo, E., ... Nyssen, J. (2014). Analyzing runoff processes through conceptual hydrological modelling in the Upper Blue Nile basin,

- Ethiopia. *Hydrology and Earth System Sciences Discussions*, 11(5), 5287–5325. doi:10.5194/hessd-11-5287-2014
- Easton, Z. M., Fuka, D. R., Walter, M. T., Cowan, D. M., Schneiderman, E. M., & Steenhuis, T. S. (2008). Re-conceptualizing the soil and water assessment tool (SWAT) model to predict runoff from variable source areas. *Journal of Hydrology*, 348(3-4), 279–291. doi:10.1016/j.jhydrol.2007.10.008
- Fenicia, F., Zhang, G. P., Rientjes, T., Hoffmann, L., Pfister, L., & Savenije, H. H. G. (2005). Numerical simulations of runoff generation with surface water-groundwater interactions in the Alzette river alluvial plain (Luxembourg). *Physics and Chemistry of the Earth*, 30(4-5 SPEC. ISS.), 277–284. doi:10.1016/j.pce.2004.11.001
- Gumindoga, W., Rientjes, T. H. M., Haile, a. T., & Dube, T. (2015). Predicting streamflow for land cover changes in the Upper Gilgel Abay River Basin, Ethiopia: A TOPMODEL based approach. *Physics and Chemistry of the Earth, Parts A/B/C*. doi:10.1016/j.pce.2014.11.012
- Habib, E., Haile, A. T., Sazib, N., Zhang, Y., & Rientjes, T. (2014). Effect of Bias Correction of Satellite-Rainfall Estimates on Runoff Simulations at the Source of the Upper Blue Nile. *Remote Sensing*, 6(7), 6688–6708. doi:10.3390/rs6076688
- Haile, a. T., Rientjes, T. H. M., Habib, E., Jetten, V., & Gebremichael, M. (2011). Rain event properties at the source of the Blue Nile River. *Hydrology and Earth System Sciences*, 15(3), 1023–1034. doi:10.5194/hess-15-1023-2011
- Haile, A. T., Habib, E., Elsaadani, M., & Rientjes, T. (2012). Inter-comparison of satellite rainfall products for representing rainfall diurnal cycle over the Nile basin. *International Journal of Applied Earth Observation and Geoinformation*, 21(1), 230–240. doi:10.1016/j.jag.2012.08.012
- Haile, A. T., Habib, E., & Rientjes, T. (2013). Evaluation of the climate prediction center (CPC) morphing technique (CMORPH) rainfall product on hourly time scales over the source of the Blue Nile River. *Hydrological Processes*, 27(12), 1829–1839. doi:10.1002/hyp.9330
- Haile, A. T., Rientjes, T., Gieske, A., & Gebremichael, M. (2009). Rainfall variability over mountainous and adjacent lake areas: The case of Lake Tana basin at the source of the Blue Nile River. *Journal of Applied Meteorology and Climatology*, 48(8), 1696–1717. doi:10.1175/2009JAMC2092.1
- Hong, Y., Adler, R. F., Hossain, F., Curtis, S., & Huffman, G. J. (2007). A first approach to global runoff simulation using satellite rainfall estimation. *Water Resources Research*, 43(8), n/a–n/a. doi:10.1029/2006WR005739
- Janssen, P. H. M., & Heuberger, P. S. C. (1995). Calibration of process-oriented models. *Ecological Modelling*, 83(1-2), 55–66. doi:10.1016/0304-3800(95)00084-9
- K. S. Abdo, B. M. Fiseha, T. H. M. Rientjes, A. S. M. G. andbA. T. H. (2009). Assessment of climate change impacts on the hydrology of Gilgel Abay catchment in Lake Tana basin, Ethiopia. *HYDROLOGICAL PROCESSES*, 23(3661–3669 (2009)). doi:10.1002/hyp
- Kebede, S. (2013). *Groundwater in Ethiopia*. doi:10.1007/978-3-642-30391-3
- Kotsiantis, S. E. (2006). Filling Missing Temperature Values in Weather Data Banks. *IEEE Conference*, 1(1), 327–334. doi:10.1049/cp:20060659
- Li, H., Zhang, Y., Vaze, J., & Wang, B. (2012). Separating effects of vegetation change and climate variability using hydrological modelling and sensitivity-based approaches. *Journal of Hydrology*, 420-421, 403–418. doi:10.1016/j.jhydrol.2011.12.033
- Lyon, S. W., McHale, M. R., Walter, M. T., & Steenhuis, T. S. (2006). The impact of runoff generation mechanisms on the location of critical source areas. *Journal of the American Water Resources Association*, 42(3), 793–804. doi:10.1111/j.1752-1688.2006.tb04493.x
- Muhammed, A. H. (2012). *Satellite Based Evapotranspiration Estimation and Runoff Simulation : a Topmodel Application To the Gilgel Abay Catchment*. Unpublished Thesis, University of Twente Faculty of Geo

Information Science and Earth Observation. Retrieved from
http://www.itc.nl/Pub/Home/library/Academic_output/AcademicOutput.html?p=13&y=12&l=20

- Nair, S., Srinivasan, G., & Nemani, R. (2009). Evaluation of Multi-Satellite TRMM Derived Rainfall Estimates over a Western State of India. *Journal of the Meteorological Society of Japan*, 87(6), 927–939. doi:10.2151/jmsj.87.927
- Narapusetty, B., Delsole, T., & Tippett, M. K. (2009). Optimal estimation of the climatological mean. *Journal of Climate*, 22(18), 4845–4859. doi:10.1175/2009JCLI2944.1
- Pearce, a. J., Stewart, M. K., & Sklash, M. G. (1986). Storm Runoff Generation in Humid Headwater Catchments: 1. Where Does the Water Come From? *Water Resources Research*, 22(8), 1263. doi:10.1029/WR022i008p01263
- Qin, Y., Chen, Z., Shen, Y., Zhang, S., & Shi, R. (2014). Evaluation of satellite rainfall estimates over the Chinese Mainland. *Remote Sensing*, 6(11), 11649–11672. doi:10.3390/rs6111649
- Reggiani, P. (2012). Representative Elementary Watershed Model User Manual, 1–90.
- Reggiani, P., & Rientjes, T. H. M. (2005). Flux parameterization in the representative elementary watershed approach: Application to a natural basin. *Water Resources Research*, 41(4), 1–18. doi:10.1029/2004WR003693
- Reggiani, P., & Schellekens, J. (2003). Modelling of hydrological responses: The representative elementary watershed approach as an alternative blueprint for watershed modelling. *Hydrological Processes*, 17(18), 3785–3789. doi:10.1002/hyp.5167
- Reggiani, P., Sivapalan, M., & Hassanizadeh, S. M. (2000). Conservation equations governing hillslope responses: Exploring the physical basis of water balance. *Water Resources Research*, 36(7), 1845. doi:10.1029/2000WR900066
- Reggiani, P., Sivapalan, M., Hassanizadeh, S. M., & Gray, W. G. (2001). Coupled equations for mass and momentum balance in a stream network: theoretical derivation and computational experiments. *Proceedings of the Royal Society A: Mathematical, Physical and Engineering Sciences*, 457(2005), 157–189. doi:10.1098/rspa.2000.0661
- Reggiani, P., Sivapalan, M., Hassanizadeh, S. M., Sivapalan, M., Gray, W. G., & Majid Hassanizadeh, S. (1999). A unifying framework for watershed thermodynamics: Constitutive relationships. *Advances in Water Resources*, 23(1), 15–39. doi:10.1016/S0309-1708(99)00005-6
- Reggiani, P., Sivapalan, M., & Majid Hassanizadeh, S. (1998). A unifying framework for watershed thermodynamics: Balance equations for mass, momentum, energy and entropy, and the second law of thermodynamics. *Advances in Water Resources*, 22(4), 367–398. doi:10.1016/S0309-1708(98)00012-8
- Rientjes, T. H. M., Haile, a. T., Kebede, E., Mannaerts, C. M. M., Habib, E., & Steenhuis, T. S. (2011). Changes in land cover, rainfall and stream flow in Upper Gilgel Abbay catchment, Blue Nile basin - Ethiopia. *Hydrology and Earth System Sciences*, 15(6), 1979–1989. doi:10.5194/hess-15-1979-2011
- Rientjes, T. H. M., Muthuwatta, L. P., Bos, M. G., Booij, M. J., & Bhatti, H. a. (2013). Multi-variable calibration of a semi-distributed hydrological model using streamflow data and satellite-based evapotranspiration. *Journal of Hydrology*, 505, 276–290. doi:10.1016/j.jhydrol.2013.10.006
- Rientjes, T. H. M., Perera, B. U. J., Haile, a. T., Reggiani, P., & Muthuwatta, L. P. (2011). Regionalisation for lake level simulation - The case of Lake Tana in the Upper Blue Nile, Ethiopia. *Hydrology and Earth System Sciences*, 15(4), 1167–1183. doi:10.5194/hess-15-1167-2011
- Sawunyama, T., & Hughes, D. A. (2008). Application of satellite-derived rainfall estimates to extend water resource simulation modelling in South Africa. *Water SA*, 34(1), 1–9. doi:0378-4738
- Schaefli, B., & Gupta, H. V. (2007). Do Nash values have value? *Hydrological Processes*. doi:10.1002/hyp

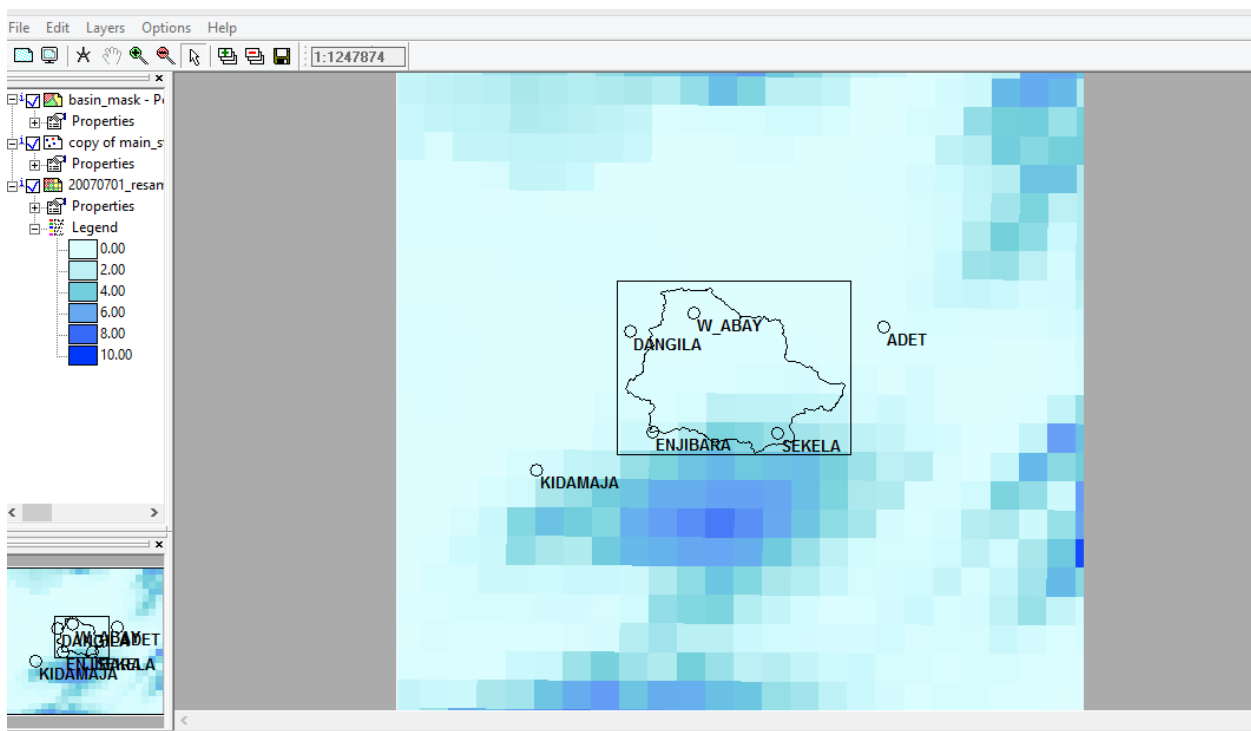
- Stisen, S., & Sandholt, I. (2010). Evaluation of remote-sensing-based rainfall products through predictive capability in hydrological runoff modelling. *Hydrological Processes*, 24(7), 879–891. doi:10.1002/hyp.7529
- Taddele, Y. D. (2009). *Hydrological Modeling to Assess Climate Change Impact at Gilgel Abay River, Lake Tana Basin – Ethiopia*.
- Tarboton, D. G. (2003). *Rainfall -Runoff Processes*.
- Tarboton, D. G., Bras, R. L., & Rodriguez-Iturbe, I. (1991). On the extraction of channel networks from digital elevation data. *Hydrological Processes*, 5(1), 81–100. doi:10.1002/hyp.3360050107
- Uhlenbrook, S., Mohamed, Y., & Gragne, a. S. (2010). Analyzing catchment behavior through catchment modeling in the Gilgel Abay, upper Blue Nile River basin, Ethiopia. *Hydrology and Earth ...*, 14(10), 2153–2165. doi:10.5194/hess-14-2153-2010
- Wale, A. (2008). *Hydrological Balance of Lake Tana Upper Blue Nile Basin, Ethiopia*.
- Walter, M. T., Mehta, V. K., Marrone, A. M., Boll, J., Gérard-Marchant, P., Steenhuis, T. S., & Walter, M. F. (2004). Errata for “Simple Estimation of Prevalence of Hortonian Flow in New York City Watersheds.” *Journal of Hydrologic Engineering*, 9(1), 70–70. doi:10.1061/(ASCE)1084-0699(2004)9:1(70)
- Yihun Taddele, Berndtsson, R., & Setegn, S. G. (2013). Hydrological Response to Climate Change for Gilgel Abay River, in the Lake Tana Basin - Upper Blue Nile Basin of Ethiopia. *PLoS ONE*, 8(10), 12–17. doi:10.1371/journal.pone.0079296
- Zhang, G. (2007). *Modelling Hydrological Response at the Catchment Scale*. UNESCO-IHE, Netherlands.
- Zhang, G. P., Fenicia, F., Rientjes, T. H. M., Reggiani, P., & Savenije, H. H. G. (2005). Modeling runoff generation in the Geer river basin with improved model parameterizations to the REW approach. *Physics and Chemistry of the Earth*, 30(4-5 SPEC. ISS.), 285–296. doi:10.1016/j.pce.2004.11.002
- Zhang, G. P., Savenije, H. H. G., Fenicia, F., & Pfister, L. (2006). Modelling subsurface storm flow with the Representative Elementary Watershed (REW) approach: application to the Alzette River Basin. *Hydrology and Earth System Sciences Discussions*, 3(1), 229–270. doi:10.5194/hessd-3-229-2006

APPENDICES

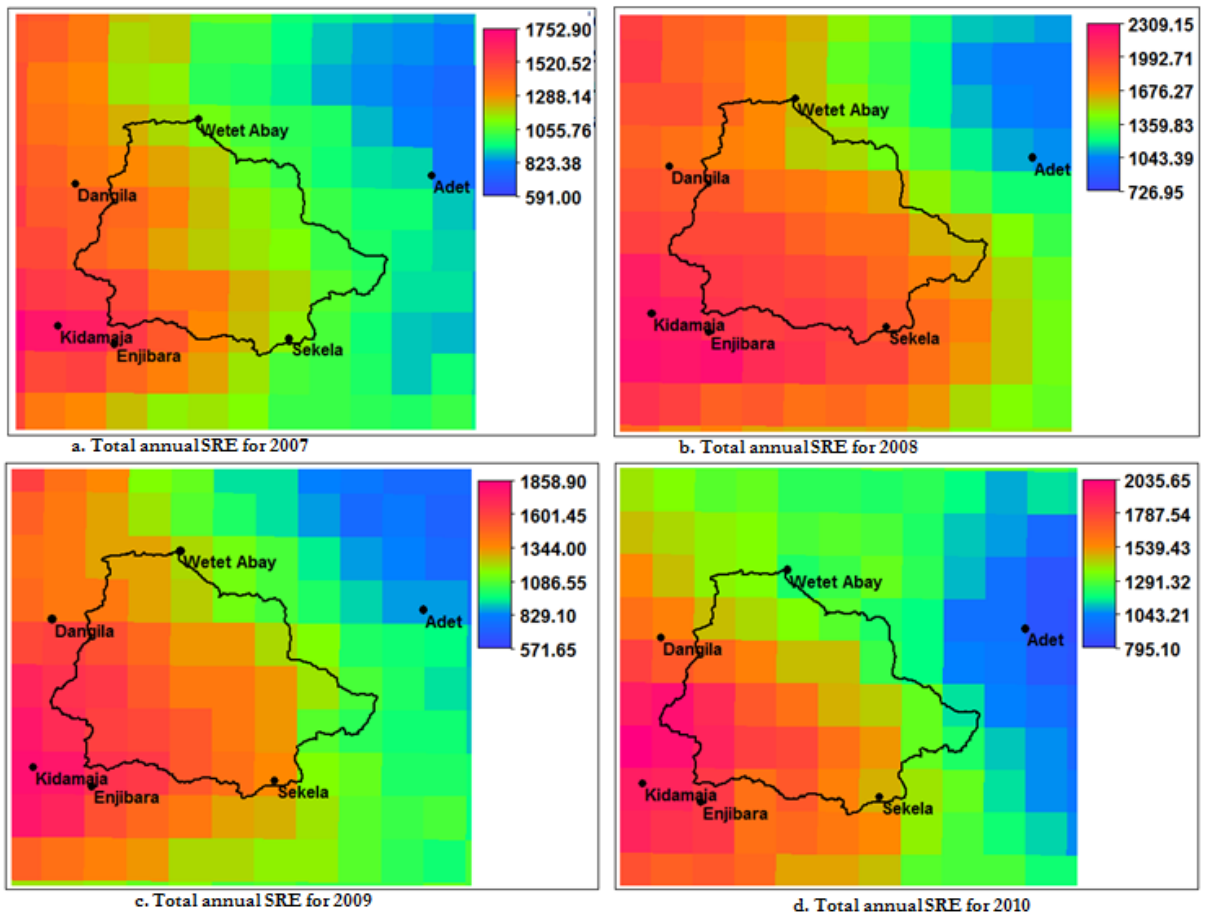
Appendix I: List of Acronyms

DEM	Digital Elevation model
ILWIS	Integrated Land and Water Information System
NSE	Nash-Sutcliffe Efficiency
RECs	Representative Elementary Columns
REW	Representative Elementary Watershed
RVE	Relative volumetric error
SREs	Satellite rainfall estimates
SRTM	Shuttle Radar Topographic Mission
TSV	Time and space variant
Y	Combination function of NSE and RVE

Appendix II: SREs Extraction based on location of gauging stations



Appendix III: spatial variation rainfall for the years 2007-2010



Appendix IV: an example of Interpolated bias factor map

